Russian Chemical Reviews **69** (6) 523 – 549 (2000) © 2000 Russian Academy of Sciences and Turpion Ltd

DOI 10.1070/RC2000v069n06ABEH000592

Structure and properties of polymers in terms of the fractal approach

V U Novikov, G V Kozlov

Contents

I.	Introduction	523
II.	Fractal analysis of the polymer structure	523
III.	Modelling of the structure and properties of polymers	537
IV.	Experimental determination of the fractal dimension	544
V.	Conclusion	546

Abstract. The review considers various manifestations of fractality in the description of the synthesis of macromolecules and the formation of the quasi-equilibrium state in polymers, fluctuation free volume, macromolecular frameworks, order parameters, and dissipative structures, acting as centres of shear stress in clusters. The possibility of numerical modelling of the properties of network polymers within the framework of fractal formalism is demonstrated. The methods for determination of the fractal dimension are described. The bibliography includes 248 references.

I. Introduction

The use in investigations of only Euclidean geometry, which describes objects with integer dimensions, restricts the possibility of adequate description of real (both natural and artificial) objects because it leaves numerous objects with fractional (fractal) dimensions beyond the scope of consideration. The properties of such objects can be described using fractal geometry.[1,2]

Frequently encountered natural and synthetic polymers belong to the class of fractal objects. A polymer consists of long-chain macromolecules. Owing to this structure, polymers possess properties differing from those of other classes of solids. The most important parameters characterising a macromolecular chain are length and rigidity.[3–5]

The structure of a vitreous polymer is thermodynamically unstable. Thermodynamically nonequilibrium processes result in the formation of fractal structures.[6] A classical example supporting this statement is a fractured surface of a polymer. It has been found experimentally that the fractal properties of a fractured surface do not depend on the thermodynamic state of the solid.[7] This is due to the thermodynamically nonequilibrium character of the fracture process.[8] In the syntheses of polymers in solution (which is the most widely used variant [9]) the main structural unit is a macromolecular coil, which is known [10] to be a fractal. To describe an object in terms of Euclidean geometry, only one parameter, namely, the Euclidean dimension d, is needed, whereas description of fractal objects requires at least three parameters: the dimension d and the Hausdorff and spectral (fracton, d_s) dimensions.[11] Thus, the question of whether or not the methods of fractal analysis should be used to describe the structure of a macromolecular coil and a polymer is not a matter of researcher's choice but is dictated by the requirements of correct approach to the problem.†

The methods of fractal analysis and the models of irreversible aggregation provide a new understanding of the processes of synthesis and provide results which are difficult to obtain (or cannot be obtained) by other methods. All the foregoing has stipulated the scope of this review the purpose of which is to summarise the results of the use of fractal approach to the synthesis and analysis of the structures and properties of vitreous polymers.

II. Fractal analysis of the polymer structure

1. A model and the structure of a macromolecular coil

In order to develop a physically substantiated description for processes such as flocculation, polymerisation, *etc*., various irreversible aggregation models, based on the physical pattern of formation of larger objects from smaller ones, have been developed.[15–18] The necessity of using models of this type in this review is due to the fact that the processes they describe result in the formation of fractal objects.

The fractal dimension of a macromolecular coil in solution (D) is determined by two types of interaction: interactions of the coil elements with one another and solvent – polymer interactions.[19] These types of interaction have been considered in detail.[20] In particular, the D value was found to depend on the chain rigidity, characterised by the Kuhn segment length (A). Linear $D(A)$ dependences have been found for flexible-, semirigid- and rigid-chain polymers (Fig. 1). An increase in the chain rigidity (an increase in A) is accompanied by a decrease in D; this implies transition to less compact macromolecular coils.[10,21] The D values obtained by extrapolation to $A = 0$ are different. The lowest value is obtained for rigid-chain polymers, which reflects the difficulty of formation of macromolecular coils in this case.[22]

For flexible- and semirigid-chain polymers, the $D(A)$ plot at $A = 0$ extrapolates to $D = 2$, which corresponds to the dimension of the coil in a Θ-solvent.[20] Thus, only a hypothetical absolutely

V U Novikov Moscow State Open University, ul. P Korchagina 22/2, 129805 Moscow, Russian Federation.
Fax (7-095) 283 80 71. E-mail: vknovik@cityline.ru
G V Kozlov Kabardino-Balkarian State University, ul. Chernyshevskogo 173, 360004 Nal'chik, Russian Federation.
Fax (7-866) 225 44 75. Tel. (7-866) 222 41 44

Received 12 April 2000
Uspekhi Khimii **69** (6) 572 – 599 (2000); translated by Z P Bobkova

† The required concepts and definitions which reflect the specific features of the results outlined below can be found in Refs 12 – 14.

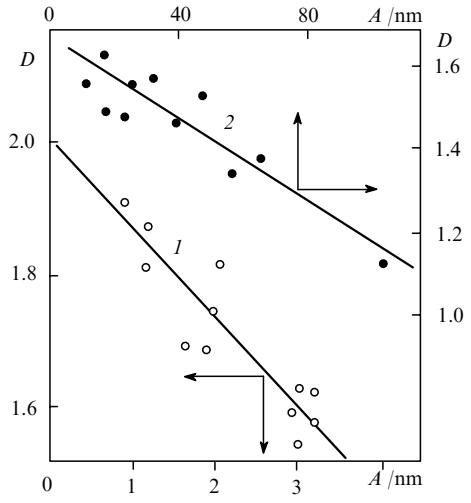


Figure 1. Fractal dimension D of a macromolecular coil *vs.* length of the Kuhn segment A for flexible- and semirigid-chain (correlation coefficient 0.82) (*1*) and rigid-chain polymers (correlation coefficient 0.85) (*2*).

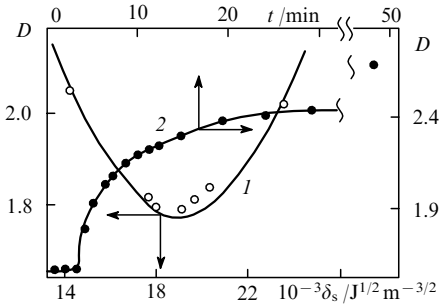


Figure 2. Fractal dimension D of a macromolecular coil for polyarylate *vs.* solubility parameter δ_s of the solvent used in the synthesis (*1*) and *vs.* reaction time t (*2*).

flexible macromolecule ($A = 0$) can have an ideal conformation in a good solvent. In real polymer chains (for $A > 0$, *i.e.* actually, for an isolated macromolecular coil), this conformation can be attained by choosing a solvent which would counterbalance the effect of excluded volume.[19] A similar extrapolation to $A = 0$ for rigid-chain polymers gives $D \simeq 1.67$. This corresponds to the dimension of a coil in a good solvent.[10] However, it should be noted that for these polymers, Θ-conditions can be created when the index in the Mark – Kuhn – Houwink equation $a \neq 0.5$ (or $D \neq 2$). For instance, Θ-conditions for polyarylate have been attained [22] at $a = 0.8$, which is equivalent to $D \simeq 1.67$ in conformity with the equation

$$D = \frac{3}{1+a} \tag{1}$$

Thus, different D values obtained for the above classes of polymers by extrapolation of the $D(A)$ plot to $A = 0$ can imply different criteria for the attainment of Θ-conditions.

Two alternative analytical expressions have been reported [20, 23] for evaluation of D as a function of the molecular characteristics of a polymer, C_∞ and S (C_∞ is the characteristic ratio, which is a measure of the statistical chain flexibility [24] and S is the cross-section area of the macromolecule)

$$C_\infty = \frac{D}{3(2-D)} + \frac{4}{3}, \tag{2}$$

$$D = 2 - 4\left(\frac{2}{C_\infty S}\right)^{1/2}. \tag{3}$$

The D values determined from Eqns (2) and (3) were found to be in good agreement with those determined using Eqn (1).[20]

The polymer – solvent interactions, which also influence the D value of a macromolecular coil in solution, can be characterised in several ways. One way is to use the Huggins constant k_H, which reflects the extent of polymer – solvent interaction.[24] The equation derived in terms of this approach shows the variation of D as a function of molecular mass M of the polymer [22]

$$D = \frac{3\ln M}{\ln M + \ln(7.14k_H - 1) - \ln k_\eta - \ln k_H}, \tag{4}$$

where k_η is the constant in the Mark – Kuhn – Houwink equation.

The $D(k_H^{-2})$ dependence obtained experimentally [20] shows that both an increase in the rigidity and improvement of the thermodynamic quality of the solvent with respect to the polymer result in higher k_H. This in turn, decreases both k_H^{-2} and D. The correlation limits of $D(k_H^{-2})$ correspond to the range $1.5 < D < 2.286$; hence, this correlation can be used for predicting the structure of a macromolecular coil in dilute solutions.

Yet another parameter used to characterise the polymer – solvent interaction is the difference between the solubility parameters of the polymer and the solvent.[25] The plot for the variation of D of polyarylate *vs.* the solubility parameter of the solvent used in the synthesis of the polymer has a dome-like shape, typical of this type of dependence (Fig. 2, curve *1*); this confirms the increase in D (an increase in the compactness of the macromolecular coil) following deterioration of the thermodynamic quality of the solvent.

The fractal dimension of a macromolecular coil D can serve simultaneously as a measure of volume interactions of this coil: for a coil in a Θ-solvent, D equal to 2 implies the absence of these interactions (the interaction parameter $\varepsilon = 0$), $D < 2$ corresponds to repulsive interactions ($\varepsilon > 0$), and $D > 2$ means attractive interactions ($\varepsilon < 0$). A simple procedure for the determination of D is based on the equation [26]

$$D = \left(\frac{5[\eta]}{[\eta]_\Theta^{2/3}} - 3\right)\left(\frac{3[\eta]}{[\eta]_\Theta^{2/3}} - 2\right)^{-1}, \tag{5}$$

where $[\eta]$ and $[\eta]_\Theta$ are intrinsic viscosities of the polymer dissolved in an arbitrary solvent and in a Θ-solvent, respectively.

By virtue of fractal analysis, one can gain some useful information, in addition to the data on molecular hydrodynamics, from the same experimental data.[27] This statement is illustrated below by some examples.

The fractal dimension D characterises the degree of 'openness' of the fractal structure — the lower D, the more efficient the penetration of particles into a fractal cluster (the more 'accessible' is the cluster for a reaction).[28] This is expressed analytically as follows:[29]

$$Q \propto t^{(3-D)/2}, \tag{6}$$

where Q is the degree of conversion of a polymer and t is the current reaction time.

Equation (6) is the main scaling relation used to describe polymerisation kinetics.[30–37] It is noteworthy that the process cannot take place for Euclidean coils (compact globules) because for them, $D = d = 3$ and $Q = \text{const}$. It is clear than in the general case, Eqn (6) should also contain diffusion parameters and the initial reactant concentrations.

An aspect related directly to the problem of macromolecular coil structure considered here is the dependence of aggregation processes on the concentration of aggregating particles c (initial concentration c_0) in some space.[38] If the density ρ of a cluster (macromolecular coil) decreases during the growth down to the density of the surrounding medium (the polymer – monomer solution), one type of universality of diffusion-limited aggregation

(DLA) is replaced by another type, namely, the particle–cluster aggregation switches to aggregation according to the Eden model;[39] subsequently, growth of the macromolecular coil ceases, having reached the critical radius R_c.[37] This variation of ρ is possible only for fractals because their density depends on the radius of gyration R_g, which is the critical radius for them [37]

$$\rho \propto bR_g^{D-d}, \tag{7}$$

where b is a proportionality factor.

In the case of Euclidean objects, $D = d$ and ρ = const. The transition between the classes of universality considered in terms of the DLA model is preceded by yet another transition, namely, the cluster–cluster aggregation is replaced by the particle–cluster aggregation; this markedly decreases the rate of the reaction but does not stop it.[40]

In terms of the cluster–cluster DLA, the synthesis of a polymer can be described using the relation [40–42]

$$R_g \propto \left(\frac{4c_0kT}{3\eta_0 m_0}t\right)^{1/D}, \tag{8}$$

where k is the Boltzmann constant, T is temperature, η_0 is the initial viscosity of the medium, t is the reaction time, and m_0 is the mass of a unit.

An increase in D implies an increase in the degree of branching of a macromolecular coil.[22] This statement is illustrated by calculation of the spectral dimension d_s, which characterises the degree of connectivity of a fractal. The d_s value for a swollen fractal with allowance for the effect of excluded volume can be estimated from the following equation:[43]

$$D = d_s\frac{d+2}{d-2}. \tag{9}$$

Note that for linear polymers, $d_s = 1$, while for branched polymers, $d_s = 1.33$.[42,43] The coil structure formed during the synthesis largely determines the molecular mass of the polymer formed. As D increases, the coil becomes more compact and the density of the coil diminishes.[44] The main models suitable in this case include the formation of a close packing of macromolecular coils, the appearance of an entanglement network, and the description of the self-acceleration effect with allowance for the concept of free volume. According to each of these models, the increase in the viscosity in the monomer–polymer system is the main reason for the formation of a macromolecular coil.[45]

To describe the limiting regimes of the dynamics of the growth of aggregates in a reaction vessel with the initial monomer concentration c_0, the characteristic length scale ξ was introduced,[46] which determines the qualitative transition from a fractal object to a non-fractal object

$$\xi \propto c_0^{-1/(d-D)}. \tag{10}$$

The former regime is realised for $R_g \ll \xi$, for a coil density much greater than the density of the medium in the reaction vessel and for the aggregate size (the degree of polymerisation for a macromolecular coil) N; it can be written that [46]

$$N(c_0, t) \propto (c_0 t)^{D/(2+D-d)}. \tag{11}$$

The latter regime is observed when $R_g \gg \xi$, the densities of the aggregate and the medium in the reaction vessel are nearly equal, and

$$N(c_0, t) \propto c_0^{(1+d)/(d-D)}t^d. \tag{12}$$

The relationship between N and Q in terms of the irreversible aggregation models can be elucidated using the main scaling relation (6) and relation (8), in which all the parameters, except for c_0, η_0 and t, are assumed to be constant,

$$Q \propto c_0^{(D-1)/2}\eta_0^{(5-D)/2}N^{(3-D)/2}. \tag{13}$$

The resulting equation can be used to estimate the dependence of Q on t for the two regimes considered above. All these dependences are non-linear and imply an increase in the reaction rate with an increase in t, that is, a self-acceleration effect.

A possible reason for self-acceleration is interpenetration of macromolecular coils compressed to the Θ-size with the formation of a stable network of molecular entanglements.[47,48] In some cases, under certain conditions of synthesis, in particular, for low c_0 and η_0, the absence of self-acceleration is assumed.[45]

It should be noted that the above variant for the calculation of $Q(t)$ does not take into account the exhaustion of the monomer during the reaction. Exhaustion of the monomer appreciably decreases the reaction rate. In other words, the effects of self-acceleration and exhaustion of the monomer act in the opposite directions. When c_0 values are low, the latter effect can suppress the former one.

An important process occurring during the synthesis of polymers is gelation; traditionally, it attracts considerable attention. However, there are several definitions of the gelation point and several methods for locating it on the $Q(t)$ curve. For example, the gelation point is found as the point in which the solution starts to exhibit some properties of a solid (elasticity, fragility, *etc.*).[48] In polymer syntheses, transition from the initial stage of polymerisation to the self-acceleration stage is referred to as gelation point.[49] The concept of gelation point used in polymer physics implies the point where the cluster which tightens the system (and extends from one system edge to the other) is formed.[36] Kolb and Herrmann [50] calculated the gelation point on the $Q(t)$ curve in terms of an approach based on the DLA models. Different approaches and different definitions of gelation cause uncertainty in its interpretation.

If the gelation effect is interpreted as the formation of a cluster tightening the system, the parameters describing this system change substantially.[36] Thus the velocity υ of the migration of clusters (macromolecular coils) with mass m is assumed to be [50]

$$\upsilon = m^{\alpha}, \tag{14}$$

where α is a scaling index.

At the point of gelation, the sign of α changes from negative to positive. This means that below the gelation point, smaller clusters are more mobile, whereas after the gelation point, the tightening cluster has the highest mobility.

Statistical geometric characteristics of the system also change in the gelation point. It has been shown both theoretically and experimentally [36] that D values of about 1.6–2.1, typical of a macromolecular coil in a solution, increase to ~2.5 (see Ref. 21), which is a value characterising a Witten–Sander cluster.[15] In terms of the cluster–cluster DLA, the time dependence of R_g is written as [51]

$$R_g \propto t^{1/z}, \tag{15}$$

where the index z is related to D and α by the expression

$$z = D(1-\alpha) - (d-2). \tag{16}$$

Polymeric systems are often described using the size distribution function of clusters (macromolecular coils). In the physical chemistry of polymers, this function is defined as the molecular-mass distribution (MMD) function. The fractal dimension D provides little information on aggregation (polymerisation); this is a static value which does not describe the aggregation dynamics. In addition, D characterises the geometric properties of only one cluster (macromolecular coil) and cannot be used to describe sets of clusters in the system. For this purpose, one has to study the cluster size distribution function $n_s(t)$, where n_s is the number of clusters consisting of s units at time t.[52]

The description of the cluster size distribution in the cluster–cluster DLA model has been analysed.[40,50,52,53] This model is completely suitable, for example, for the description of polymerisation of polymethyldiammonium chloride (PMDAC). The D value of this polymer, estimated to be 1.65 using Eqn (1), is a typical fractal dimension of aggregates formed during the clus-

ter–cluster DLA.[37] In view of this fact, the molecular mass distribution of PMDAC is described using the function [52]

$$n_s(t) \propto s^{-2}t^z. \quad (17)$$

Let us consider methods used to estimate the parameters appearing in relation (17). The $n_s(t')$ values for the gelation point are found from the experimental MMD curves, $W_i(N)$, in the following way. It is assumed that $N = s$ and the part of the polymer corresponding to s_i is roughly equal to the total weight proportion of the polymer fraction W_i. By dividing W_i into s_i and by multiplying the ratio by the maximum degree of conversion Q_i, we obtain the $n_s(t')$ value. The index z is found from Eqn (16). In terms of the DLA model, the diffusion coefficient D_s is usually represented, by analogy with Eqn (14), in the form[51, 52]

$$D_s \propto s^{\alpha}. \quad (18)$$

In view of the definition of D_s (see Ref. 54), it can be easily found from Eqn (18) that

$$\alpha \propto -\ln \eta_0. \quad (19)$$

It was shown [51, 52] that α determines the pattern of the MMD function. For $\alpha < -0.5$, dome-shaped distribution curves having a maximum were obtained, and for $\alpha > -0.5$, the curves decay monotonically. The MMD curves for PMDAC are also dome-shaped. If we assume the equality sign in relation (19), α would vary from -1 to -3, which completely complies with the experimental MMD curves. The position of the MMD maximum N_{max} is determined by the relation [55]

$$N_{max} \propto \frac{-\alpha}{1-\alpha}. \quad (20)$$

An increase in c_0 results in an increase in η_0 as well as in α and N_{max}.

Figure 3 presents the variation of $\ln(s^2n_s)$ *vs.* $\ln(st^z)$ for PMDAC samples synthesised at different c_0. It can be seen that all experimental points fit in one curve. This is the most important result which confirms the legitimacy of using irreversible aggregation models for the description of polymerisation.

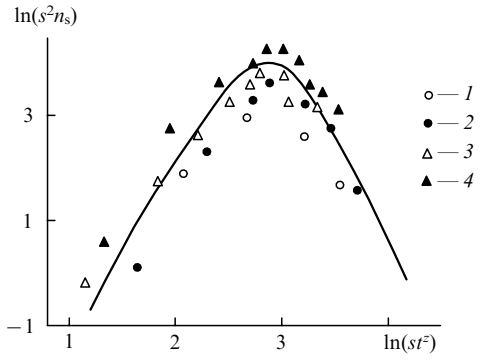


Figure 3. Generalised MMD curve as the function $\ln(s^2n_s)$ *vs.* $\ln(st^z)$ for PMDAC synthesised at c_0 of 1.0 (*1*), 2.5 (*2*), 4.0 (*3*) and 5.0 (*4*) mol litre^{-1}.

The general curve shown in Fig. 3 can be used to predict the kinetics of MMD as a function of t. For this purpose, the $s = N$ value is first specified and the st^z value is determined for an arbitrary t. After that, the corresponding s^2n_s value is found using the plot in Fig. 3 and then W_i is calculated. The same calculation should be repeated for a different s, and so on.

The relationship between the structures of the macromolecular coil and a solid polymer and its influence on the glass transition temperature T_g have been analysed in relation to a series of vitreous amorphous copolymers — aromatic copolyestersulfonoformals (APESF). Transition to the condensed state implies a change in the environment of a macromolecular coil; the solvent molecules surrounding the coil are replaced by similar coils. This changes the fractal dimension of the coil [44] and, correspondingly, the fractal dimension of the polymer structure as a whole.[56]

To derive an analytical expression representing the relationship between the structure and properties of polymers, a definite quantitative model of the structure is required. The cluster model for the structure of the amorphous state of polymers was used for this purpose.[57] This model is based on the concept of local (short-range) order. The proportion of segments densely packed in the clusters φ_{cl} is a parameter of order, which is related to T_g by the following expression:[58]

$$\varphi_{cl} \simeq 0.03(T_g - T)^{0.55}, \quad (21)$$

where T is the testing temperature.

Within the framework of the cluster model, the glass–liquid transition is regarded as the thermofluctuational decomposition of clusters at $T = T_g$.[59] Fractal concepts are interrelated with the cluster model; the relationship between the main characteristics of these models is given in the form [60]

$$d_f = d - 6\left(\frac{\varphi_{cl}}{SC_\infty}\right)^{1/2}, \quad (22)$$

where d_f is the fractal dimension of the supermolecular (supersegmental) structure of the polymer

$$d_f = (d-1)(1+\mu), \quad (23)$$

where μ is the Poisson coefficient.

The S values for the sulfone and formal fragments which constitute APESF were assumed to be 35 and 23 Å^2, respectively,[48] and S values for copolymers were estimated using the condition of additivity. The C_∞ values were calculated from the equation [60]

$$C_\infty = \frac{d_f}{d(d-d_f)+4/3}. \quad (24)$$

Using Eqns (21)–(24), one can calculate T_g proceeding only from the structure of the macromolecular coil in solution, which is characterised by D, and from the molecular parameter S. The T_g values calculated by this procedure are in good agreement with experimental values; the discrepancy between them does not exceed 4% (Fig. 4).

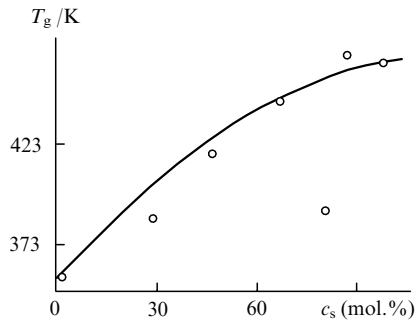


Figure 4. Glass transition temperature T_g *vs.* the content of sulfone fragment. The curve corresponds to experimental results and the points are calculated values.[14]

2. Hierarchy and evolution of dissipative structures in polymers

In recent years, principles of synergetics of nonequilibrium systems and fractal analysis have been used to study the relationship between the structures and properties of vitreous polymers,[61–64] because an amorphous polymer is a thermodynamically nonequilibrium system.

The main feature distinguishing polymers from other classes of solids is that they consist of long-chain macromolecules. Therefore, it is natural to assume that the structural hierarchy of polymers (including network polymers) should be based on their molecular structure. In recent years, the characteristic ratio C_∞ has been used more and more frequently as a molecular parameter to describe the properties of polymers, instead of some other characteristics such as a/σ (a is the chain 'thickness' and σ is the chain rigidity).[65,66] According to Boyer and Miller,[67] this is due to the fact that σ has greater uncertainty than C_∞. Indeed, σ depends on the bond angles in the macromolecule, while C_∞ depends on the bond lengths, which are normally determined much more precisely than the bond angles. Without objecting to the legitimacy of this conclusion, we believe, nevertheless, that the reasons for the wide use of the parameter C_∞ are much more fundamental (see, for example, a number of studies [60–64,68–71]). This can be demonstrated in relation to the epoxy polymers based on bisphenol A and cured by diamine (EP-1) and anhydride (EP-2). For example, to estimate the Bragg interval d_B for these polymers, wide-angle X-ray diffractometry has been used.[71] The resulting value was used to determine the diameter ø (and, hence, the cross-section area S) of the molecule, simulated by a cylinder, from the following relation:

$$ø \approx 1.22\, d_B. \tag{25}$$

Subsequently, using the empirical relation [71]

$$T_g \approx 129\left(\frac{S}{C_\infty}\right)^{1/2}, \tag{26}$$

where T_g is expressed in Kelvins and S is expressed in Å^2, one can calculate the C_∞ values for epoxy polymers.

The behaviour of a solid subjected to mechanical treatment is determined by the processes of formation (disintegration) and evolution of dissipative structures (DS), which ensure the optimum mode of dissipation of the supplied energy.[60,72,73] This general statement is valid for all polymers. Polymers have local order, which occurs as DS.[74,75] However, direct application of the fundamental principles of thermodynamics and statistical physics of nonequilibrium systems to the investigation of the deformation of materials of a particular class is often difficult or even impossible without the knowledge of a definite quantitative model for the structure of this material. In the case of amorphous polymers, the cluster model is suitable for this purpose.[57,74]

A specific feature of the DS formed in polymers is the existence of a universal hierarchy of space scales (structural levels), which is also reflected in the hierarchy of linear dimensions of the structure.[60,63] Even elastically isotropic solids are characterised by at least three independent length scales, l_1, l_2 and l_3, which are related to one another [73]

$$l_1 = a, \tag{27}$$

$$l_2 = a\Lambda_0, \tag{28}$$

$$l_3 = a\Lambda_0\Lambda_i, \tag{29}$$

where a is the minimum scale, Λ_0 and Λ_i are automodelling coefficients.

When choosing these length scales as applied to polymers, one should reject the atomic-size level because a polymer consists of long macromolecules. Therefore, the bond length in the macromolecular backbone l_0, which is of the order of several angstroms, should be taken as the minimum scale a for polymers.[62,76] Then the next (segmental) structural level would be determined by the length of statistical segment l_{st}, which is found from the equation

$$l_{st} = l_0 C_\infty.$$

Hence, provided that $l_1 = l_0$, it can be written for this structural level that [77–79]

$$\Lambda_0 = C_\infty.$$

The next structural level for polymers is the topological level, the parameters of which are determined by characteristics of the network of macromolecular entanglements ('loops') in linear polymers or the network of chemical cross-links in cross-linked polymers. The characteristic length for this level is the distance between the entanglement points or chemical cross-linking points R_s

$$R_s = 18\left(\frac{2V_{cl}}{F}\right)^{-1/3}, \tag{30}$$

where V_{cl} is the density of the cluster network of entanglements, F is the cluster functionality.

If the equality $\Lambda_0 = C_\infty$ is retained for the subsequent structural levels, Eqns (27)–(29) for polymers can be written in the form

$$l_1 = l_0, \tag{31}$$

$$l_2 = l_{st} = l_0 C_\infty, \tag{32}$$

$$l_3 = R_s = l_0 C_\infty^2. \tag{33}$$

Figure 5 shows the dependence of R_s *vs* C_∞^2. Splitting of the plot into two straight lines is due, first, to the great scatter of the published data [62,76,80] and, second, to different approaches to the interpretation of the $l_2 = l_{st}$ value.[62,81] Nevertheless, the fact that R_s is proportional to C_∞^2 confirms that C_∞ is the automodelling coefficient for the transition of the scale of DS dimensions from l_{st} to R_s.

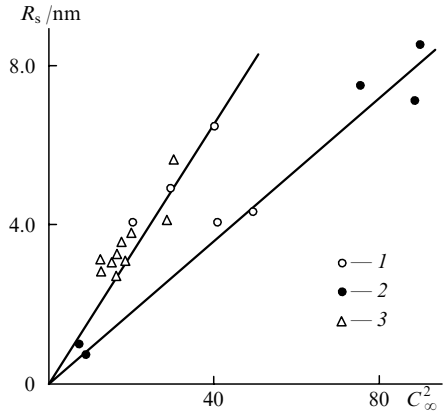


Figure 5. Distance between entanglements (chemical cross-linking points) *vs*. characteristic ratio for amorphous vitreous (*1*), amorphous-crystalline (*2*) and cross-linked (*3*) polymers.[79]

Figure 6 illustrates the relationship between the R_s values calculated from Eqns (30) and (33). Aharoni [76] noted an increase in R_s following an increase in the chain flexibility (increase in C_∞) for a large number of linear polymers

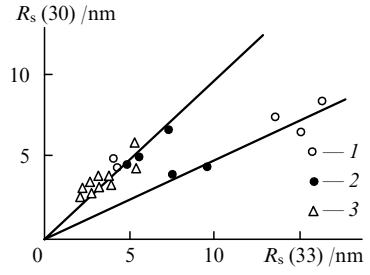


Figure 6. Relationship between the distances between entanglements (chemical cross-linking points) R_s calculated from Eqns (30) and (33) for amorphous glassy (*1*), amorphous-crystalline (*2*) and cross-linked (*3*) polymers.[79]

$$R_s \simeq 10\, C_\infty. \quad (34)$$

A similar relation holds for cross-linked polymers

$$R_s \simeq 5\, C_\infty. \quad (35)$$

Thus, the C_∞ value, which is correlated with R_s, appears to be controlled by the polymer topology, which can be varied by varying the cross-linking density v_s.

Polymers are characterised by one more, specific length scale; this is the section of a macromolecule between entanglement points or chemical cross-linking points L_s, which can be determined from the equation

$$L_s = \frac{F_{ch}}{2Sv_s}, \quad (36)$$

where F_{ch} is the functionality of a chemical cross-linking point ($F_{ch} = 4$).[14]

Figure 7 shows the variation of L_s *vs.* C_∞^3, which can be approximated by a straight line passing through the origin of coordinates. The L_s/C_∞^3 ratio has the order of l_0.[62, 76] Hence, for this structural level, typical of polymers, C_∞ can be accepted as the automodelling coefficient.[82–84]

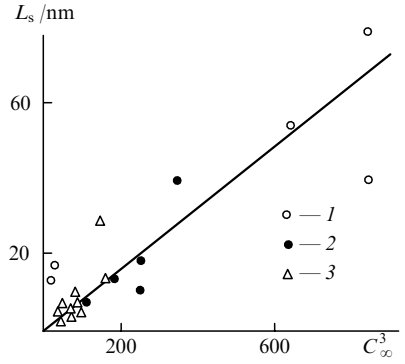


Figure 7. Length of the section of a macromolecule between entanglements (chemical cross-linking points) L_s *vs.* characteristic ratio C_∞^3 for amorphous glassy (*1*), amorphous-crystalline (*2*) and cross-linked (*3*) polymers.[79]

Let us consider the evolution of DS in network polymers during deformation. It has been shown[74] that plastic yield in amorphous polymers occurs exactly in clusters, the yield point being dependent only on the density of the cluster network of entanglements (v_{en}), *i.e.* on the number of closely packed segments in unit volume of the polymer. Yield can be regarded as the loss of stability of clusters in the field of mechanical stress, while cold flow is the deformation of a devitrified loosely packed matrix in which the role of chemical cross-links is played by the cluster network of entanglements.[85] This interpretation permits one to specify the structural changes occurring during deformation of network polymers in terms of the percolation cluster model.[60, 72–74]

As noted above, the DS formed (or existing) in a solid subjected to deformation are distinguished by a universal hierarchy of structural levels.[86] Balankin[87, 88] suggested that the hierarchical structure of the DS in a solid is based on a fundamental feature, *i.e.* shear stability, which stipulates the difference between the characteristic space scales of the regions of localisation and dissipation of energy 'pumped' into the solid on external treatment. The characteristic scale of the regions (l_s) in which excess energy is dissipated is proportional to the shear modulus G. Since, in terms of the cluster model, these regions can be associated with clusters, it is expedient to use the characteristic size l_{st} as l_s. Figure 8 illustrates the relationship between G and l_{st}, which is approximated by a straight line that passes through the origin of coordinates. This confirms the legitimacy of using l_{st} as l_s.

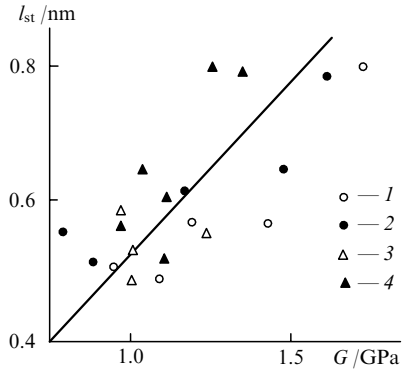


Figure 8. Relationship between the length of statistical segment l_{st} and the shear modulus G for EP-1 (*1*), EP-2 (*2*) and for EP-1 (*3*) and EP-2 (*4*) samples cured at a hydrostatic pressure of 200 MPa.[78]

With allowance for the above interpretation of cold flow and for Eqn (30), the distance between the clusters R_{cl} should be accepted as the next level in the hierarchy of structural levels. The characteristic size of the regions of localisation of the 'pumped-in' energy is

$$l_e \propto B + \frac{4}{3}G, \quad (37)$$

where B is the bulk modulus.[73] The possibility of equating R_{cl} and l_e is verified in the following way. The ratio of the space scales of the DS of adjacent structural levels, L_i and L_{i+1}, is expressed as follows:[73]

$$\frac{L_{i+1}}{L_i} = \frac{l_e}{l_s} = \left(B + \frac{4}{3}G\right)G^{-1} = \Lambda_i. \quad (38)$$

It is clear that the multiplication of the ratio $[B + (4/3)G]/G$ by l_s, which is equal to l_{st}, gives l_e. The R_{cl} value can be estimated using Eqn (30).

The dependence of l_e on $[B + (4/3)G]$ also proved to be linear (Fig. 9), which implies that the parameter l_e can, in principle, be used as the characteristic size of the regions of localisation of the pumped-in energy. However, this assumption can be ultimately confirmed by comparing l_e and R_{cl}. A correlation between these parameters has been found;[60] it was shown that R_{cl} regularly exceeds l_e by $\sim$0.8 nm. This relationship between l_e and R_{cl} can be interpreted by virtue of the cluster structure model for an amorphous polymer (Fig. 10).[89] Evidently, the decrease in R_{cl} by $\sim$0.8 nm, which is roughly equal to l_{st}, means that the pumped-in energy does not spread throughout the whole polymer bulk but is localised only in the loosely packed matrix because a cluster with the characteristic size l_{st} is excluded from consideration. Compar-

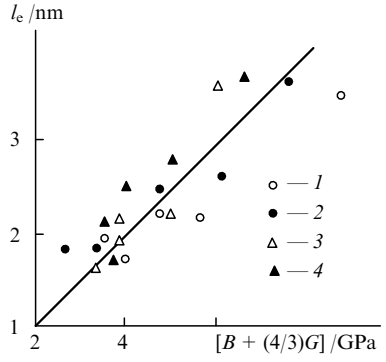


Figure 9. Relationship between the characteristic size of the regions of localisation of the pumped-in energy l_e and the parameter [B + (4/3)G]. For designations, see Fig. 8.[78]

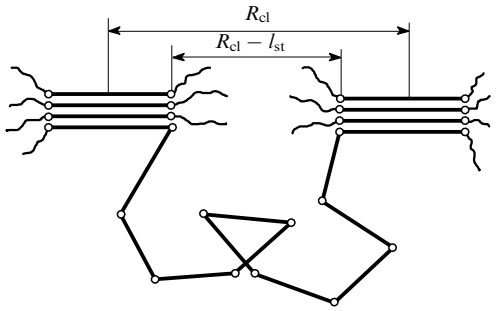


Figure 10. Parameters of the cluster structure model for an amorphous polymer.

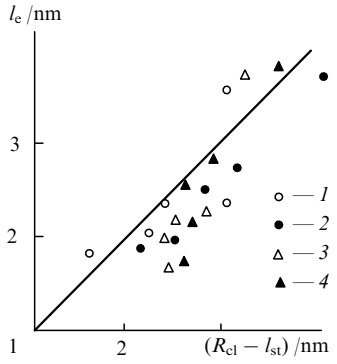


Figure 11. Relationship between the characteristic size of the regions of localisation of the pumped-in energy l_e and the $(R_{cl} - l_{st})$ value. For designations, see Fig. 8.

ison of the l_e value and the difference $R_{cl} - l_{st}$ (Fig. 11) confirms this conclusion. Hence, the structural characteristics l_e and $R_{cl} - l_{st}$, estimated within the framework of the cluster model and regarded as the space scales of the DS of adjacent levels [see Eqn (38)], allow one to estimate the automodelling coefficient for the mechanical deformation of a network polymer Λ_i, which is equal to the fractal dimension D_f of the regions of localisation of excess energy in a plastically deformed medium. In a first approximation, the D_f value can be expressed in terms of the Poisson coefficient μ in the following way:[72]

$$D_f = 2\frac{1-\mu}{1-2\mu}. \tag{39}$$

The relationship between the dimension D_f and the automodelling coefficient Λ_i for the network polymers under consideration is illustrated in Fig. 12. It can be seen that both the magnitudes

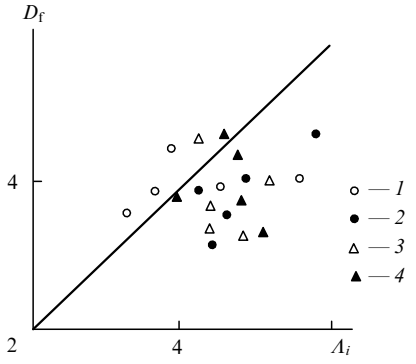


Figure 12. Relationship between the fractal dimension of the regions of localisation of excess energy D_f and the automodelling coefficient Λ_i. For designations, see Fig. 8.

and the patterns of variation for these parameters coincide. Thus, plastic yield and cold flow of network polymers are adequately described in terms of the thermodynamics of nonequilibrium processes and the cluster model of amorphous polymers provides a correct description of the structure of network polymers. It is also evident that clusters are identified as DS.

Similar results have been obtained for film samples of a linear polymer — polyarylatesulfone.[90] Using Eqn (38) and the ratio [14]

$$\frac{L_s}{l_{st}} = \left(\frac{R_s}{l_{st}}\right)^D, \tag{40}$$

it can be shown that

$$\Lambda_i = D_f \approx \left(\frac{L_s}{l_{st}}\right)^{1/D}. \tag{41}$$

Figure 13 shows that the L_s values estimated from Eqns (36) and (41) are in good agreement with each other. This implies that the sections of a macromolecule between entanglements and between clusters also obey (are controlled by) the DS hierarchy.[90]

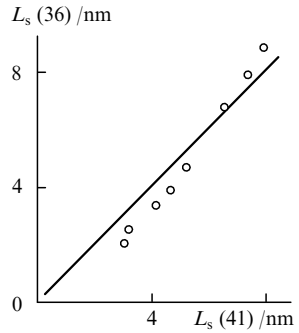


Figure 13. Relationship between the lengths of macromolecule sections between entanglements determined using Eqns (36) and (41) for polyarylatesulfone.[90]

In view of the foregoing, it can be suggested that the automodelling coefficient Λ_i in Eqn (38) is equal to C_∞. Then this equation assumes the form

$$\frac{B}{G} + \frac{4}{3} = C_\infty. \tag{42}$$

The B and G values can be expressed in terms of Young's modulus (E) and the fractal dimension of the polymer structure d_f in the following way:[91]

$$B = \frac{E}{d(d-d_f)}, \tag{43}$$

$$G = \frac{E(d-1)}{2d_f}, \tag{44}$$

where $d = 3$.

Using Eqns (42)–(44), one can estimate quantitatively the relationship between the molecular parameter C_∞ and the fractal dimension d_f.[92]

$$\frac{2d_f}{d(d-1)(d-d_f)} + \frac{4}{3} = C_\infty. \tag{45}$$

The dependences of d_f found from Eqns (23) and (45) for various classes of polymers are presented in Fig. 14. It can be seen that the results are in good agreement with each other. It is noteworthy that the methods of calculation are completely independent — Eqn (23) employs the results of mechanical testing, while Eqn (45) is based on published data for C_∞.[92]

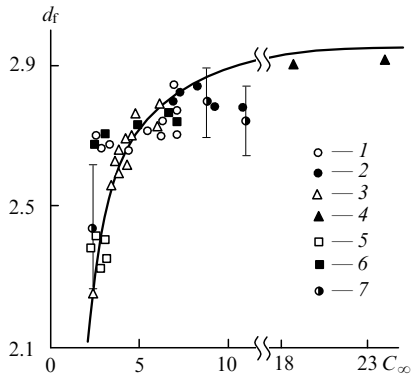


Figure 14. Fractal dimension of the structure d_f of polymers *vs.* characteristic ratio C_∞.
Solid line — calculation from Eqn (45); dots — calculation from Eqn (23): (*1*) linear polymers, impact testing; (*2*) linear polymers, calculation of d_f from the data of Ref. 60; (*3*) cross-linked epoxy polymers; (*4*) super-high-molecular-mass polyethylene produced by solid-phase extrusion; (*5*) polyarylate prepared by solid-phase extrusion at $T > T_g$; (*6*) linear polymers, stretching testing; (*7*) linear polymers, calculation of d_f from small-angle X-ray diffraction data. For sample (*7*) experimental data on the inaccuracy are given.[60]

The evolution of DS induced by various types of treatment of the polymer has been considered.[64, 93, 94] Figure 15 shows the dependence of the cluster functionality F on the curing agent : oligomer ratio (K_{st}) for epoxy polymers in deformed and non-deformed states. The most characteristic distinction between the plots being compared is the substantial increase in F after the yield point. The simultaneous decrease in V_{cl} and increase in F upon deformation of polymers up to the yield point[63, 64] implies decomposition of unstable clusters characterised by relatively low F to leave only stable clusters with large F.[95] The decay of unstable clusters induces mechanical devitrification of the loosely packed matrix; this explains the plastic behaviour of the polymer in the plateau of forced rubber-like elasticity (cold flow).[96, 97]

The opposite situation is observed during heat ageing, namely, the local order (V_{cl}) increases and the molecular mobility of chains is suppressed (D decreases).[94]

Experimental evidence for the fractality of the cluster structure (or DS) has been obtained using wide-angle X-ray diffraction analysis.[98–100] The integral intensity of the amorphous halo I_{cl} can be regarded as a measure of distributed particles (clusters), while its half-width can be taken as a measure of their effective size; the relationship between these values is illustrated in Fig. 16

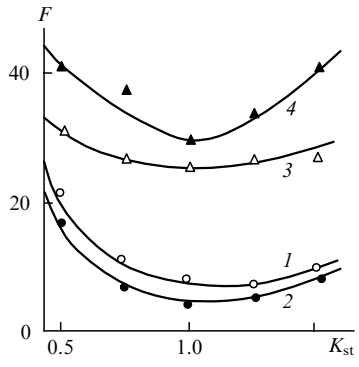


Figure 15. Functionality of clusters *vs.* the curing agent : oligomer ratio for epoxy polymers EP-1 (*1*, *3*) and EP-2 (*2*, *4*) before (*1*, *2*) and after (*3*, *4*) the yield point has been attained.

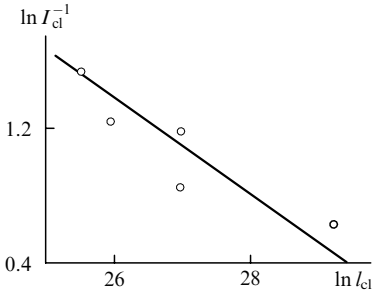


Figure 16. Reciprocal integral intensity of X-ray scattering *vs.* cluster half-width for EP-1.[98]

in relation to EP-1. The $I_{cl}^{-1}(l_{cl})$ dependence presented in the logarithmic coordinates is readily transformed into the form[98]

$$I_{cl}^{-1} \propto l_{cl}^{d_f}, \tag{46}$$

where $d_f \simeq 2.70$.

This type of dependence is typical of fractal structures; it can serve as experimental evidence confirming the fractality of the polymer structure. In addition, the d_f value is in good agreement with the fractal dimensions found for other epoxy polymers (see, for example, Ref. 69).

A fundamental description of the process of polymer fracture which includes the dilaton concept[101–103] as a constituent has been proposed.[104] The dilaton model assumes the formation of a negative density fluctuation, dilaton, the length of which is determined by the free path of phonons Λ_f. In this case, the overload factor χ on the bonds being ruptured depends on Λ_f and on the interatomic distance a_{at}:[101]

$$\chi = \frac{\Lambda_f}{a_{at}}. \tag{47}$$

The Λ_f values found for oriented polymers are about 10 nm and χ are about 30–40.[103] However, for nonoriented polymers, it was found that $\chi \leqslant 1$, *i.e.* $\Lambda_f \leqslant a_{at}$. These dilatons were called 'degenerate' (practically, this means that phonons have no free path).[105–107]

The use of the fracton concept[28] provided a fundamental interpretation for this seeming contradiction. Fractons are vibrational excitations localised on a fractal. Since the chain section between entanglements or cross-links is a fractal, a phonon localised on this section becomes a fracton. Localisation of a phonon means that it has no free path; this accounts for the fact that $\chi \leqslant 1$.

During orientation of a polymer, the chain section in question is stretched; finally, it becomes straight. In this case, its Hausdorff dimension is equal to the topological dimension

$$D = d_t = 1 \tag{48}$$

and the fractal behaviour switches to the Euclidean behaviour: the phonon becomes delocalised and acquires some free path controlled by the structure of the oriented polymer. Now $\chi > 1$. Thus, the dilaton concept is actually a specific case of the fracton theory (for $D = 1$).[104]

The following relationship between the parameters χ and D has been obtained:[104]

$$\chi \simeq D^{-2}. \tag{49}$$

An increase in the molecular mobility (increase in D) results in stress relaxation on the non-oriented polymer chains ($\chi < 1$).[108]

Since characteristics of fractal analysis are general, the relationship between the structures of different aggregation (physical) states of the polymer can be established. For example, a macromolecular coil (cluster) in solution and the polymer structure in the condensed state are fractals with the dimensions D and d_f, respectively.[44, 109] This fact can be used to predict the structure of a solid polymer even at the stage of synthesis.[110–112] The D value,

with allowance for the effect of excluded volume, is determined by Eqn (9). For linear polymers, it should be accepted that d_s in this equation is equal to 1.[43] Transition to the condensed state is accompanied by the change in the environment of a macromolecular coil; a coil becomes surrounded by similar coils instead of solvent molecules. This results in the change of the fractal dimension d_f for the condensed state [44]

$$d_f = \frac{d_s(d+2)}{2}. \quad (50)$$

For linear polymers, provided that $d_s = 1$ and $d = 3$, it follows from Eqns (9) and (50) that [111]

$$d_f = 1.5D. \quad (51)$$

Equation (51) clearly demonstrates the relationship between the coil structure in solution and the structure of the condensed polymer.

3. Quasi-equilibrium state of polymers

Neither completely ordered nor completely disordered polymers have been obtained to date. One reason for this situation is the chain nature of polymer molecules (in particular, the formation of loops during crystallisation).[113] The tendency for transition to a more equilibrated state in polymers is often attributed to an increase in the degree of ordering.[114] Therefore, it can be assumed that processes in which this tendency is manifested (for example, heat ageing, thermosetting, *etc*.) are subject to a competition of two opposing mechanisms. An increase in the degree of ordering is counteracted by the entropy of 'stretching' of macromolecules. When the thermodynamic forces of these mechanisms have been balanced, the polymer reaches some quasi-equilibrium state.[60] Perturbation of the balance in either direction governs the pattern of changes in the polymer structure. In other words, under certain conditions, a polymer can be transformed not only towards a more equilibrated state but also away from equilibrium. According to its physical essence, the latter process can be called 'antirelaxation'. Some causes and consequencies of this process are considered below in terms of the cluster model of the structure of the amorphous state of polymers and cluster analysis.

Thermosetting of extruded specimens of polyarylate occurs in the loosely packed matrix;[112] therefore, the D_f value should be taken as the fractal dimension which determines the process in a structural element (for example, in a tube). Figure 17 *a* shows the variation of the thermosetting ψ as a function of D_f for extrudates, which implies that the thermal shrinkage changes its sign when $D_f \simeq 3$. This fact is very interesting by itself. In the case of extrudates with $D_f > 3$, a less closely packed structure (having greater D_f) is transformed during relaxation (thermosetting) into a more closely packed structure (having smaller D_f), which is, therefore, closer to equilibrium. The behaviour of specimens with $D_f < 3$ requires clarification. At the first glance, it seems that as D_f decreases and the structure changes, $\psi = 0$ should imply termination of thermosetting. However, this does not occur; instead, ψ only changes its sign. This effect can be easily explained by two specific features of the cluster model — arbitrary orientation of the cluster axes in space and connection of clusters by 'interpenetrating' chains, which are subject to the limitations of the Gaussian statistics.[97] This means that it is impossible to attain a close packing of clusters, *i.e*. conditions of thermodynamic equilibrium cannot be reached in an amorphous polymer. This has been the reason for the introduction of the above-mentioned concept of 'quasi-equilibrium state',[115] in which forces due to which a polymer tends to a thermodynamic equilibrium and, hence, to an increase in the degree of local ordering are counterbalanced by entropy forces of the 'interpenetrating chains'. The last-mentioned fact can induce transition of an amorphous polymer from a thermodynamically more equilibrated state to a less equilibrated state. Experimental dependence of ψ on the draw ratio λ confirms this direction of the thermosetting process (Fig. 17 *b*).

The most characteristic feature of the relationship between D and d_f (Fig. 18) is the fact that the limiting value $D = 1$ is attained at $d_f = 2.5$ rather than at $d_f = 2$. Recalling that the dimension D characterises the mobility (deformability) of the section of a macromolecule between chemical cross-linking points (entanglement points) and $D = 1$ implies the loss of molecular mobility by this section. The quasi-equilibrium state corresponds to 'freezing' of the molecular mobility of polymer chains and, as a consequence, to the transition to brittle fracture, which is realised at $D_f < 3$.[87] Since D_f and d_f are related to each other as follows [87]

$$D_f = 1 + \frac{1}{3 - d_f}, \quad (52)$$

it can be readily seen that $d_f = 2.5$ corresponds to $D_f = 3$.

When examining the dependence of d_f on the relative portion of the loosely packed matrix φ_{lp} in poly(methyl methacrylate), high-density polyethylene, polycarbonate, and polyarylate (Fig. 19), attention is drawn by the fact that for $\varphi_{lp} = 0$ (the hypothetical state characterised by full local ordering), the d_f values are extrapolated to certain d_f^0 values (which are different for different polymers), exceeding the lower limiting value, equal to 2. Using published data for C_∞ (see, for example, Ref. 113), one can calculate the theoretical d_f^t values from Eqn (45) and compare them with the limiting d_f^0 value (see Fig. 19). The parameters d_f^t and d_f^0 are well correlated (Table 1), which reflects the occurrence of a quasi-equilibrium state. Using Eqn (45) and the relation

$$\varphi_{cl} = C_\infty l_0 S V_{cl}, \quad (53)$$

the following limits can be identified: for $C_\infty > 3$, a quasi-equilibrium state cannot be attained at all; for $C_\infty = 2-3$, it may happen that $D_f < 3$; the value $d_f = 2$, corresponding to $D_f = 2$ is reachable only for a polymer with $C_\infty = 2$. Analysis of the results obtained in terms of Eqn (45) as well as the data given in Fig. 19 and in Table 1 show that Eqn (45) determines the minimum d_f values possible for a given C_∞.

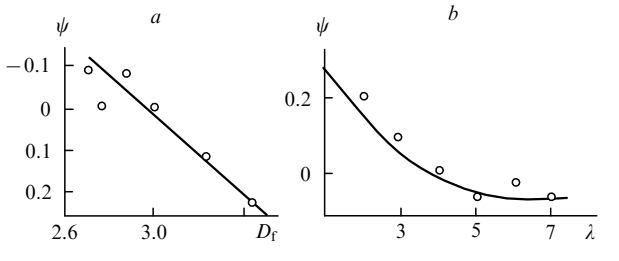


Figure 17. Thermosetting ψ *vs*. the dimension of the regions of localisation of excess energy D_f (*a*) and extrusion draw ratio λ (*b*) for polyarylate extrudates.

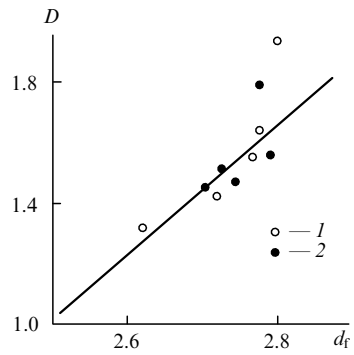


Figure 18. Relationship between the fractal dimensions of the macromolecule section between cross-linking points D and of the structure d_f for epoxy polymers EP-1 (*1*) and EP-2 (*2*).

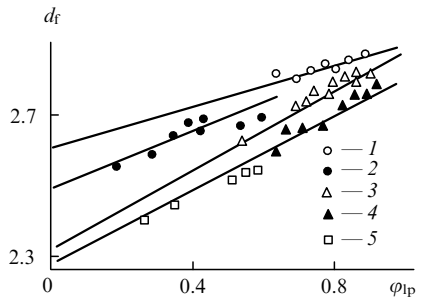


Figure 19. Fractal dimension of the structure d_f *vs.* proportion of the loosely packed matrix φ_{lp} for poly(methyl methacrylate) (*1*), high-density polyethylene (*2*), polycarbonate (*3*), polyarylate (*4*), and polyarylate extrudates (*5*).

Table 1. Fractal dimensions of the polymer structures d_f^t and d_f^0.

Polymer	d_f^t	d_f^0
Poly(methyl methacrylate)	2.55	2.60
High-density polyethylene	2.53	2.49
Polycarbonate	2.29	2.31
Polyarylate	2.23	2.27
Epoxy polymer	2.58	2.51

This accounts for the discrepancies between the d_f values found from relations (23) and (45) — the former gives the real d_f value and the latter gives the minimum possible one.

The dependences of D_f on the curing agent : oligomer ratio (Fig. 20) for EP-2 specimens immediately after the manufacture (curve *1*) and after keeping at room temperature for 1.5 years (physical ageing) (curve *2*) show that during ageing, D_f approaches 3, this effect being more pronounced for nonequilibrium systems with a deficiency or an excess of a curing agent. The minimum C_∞ value for the epoxy polymer with $K_{st} = 1.0$ is equal to 3.38.[71] With allowance for this fact, an estimate of the minimum D_f value also gave $\sim$3.38. This estimate is in good agreement with the experimental D_f value for the aged polymer ($D_f \simeq 3.16$).

The existence of the quasi-equilibrium state is also confirmed by the temperature dependences of the density fluctuations $\langle\Delta\rho/\rho\rangle^2$ (Fig. 21), which diminish as the temperature rises and tend to zero for $T = 0$, which corresponds to an ideal structure. However, there occurs a transition at temperature T^* below which $\langle\Delta\rho/\rho\rangle^2$ deviates from the predicted pattern [116] and remains constant as the temperature varies. The density fluctuations above T^* are supposed to be due to the local mobility of the sequences in the polymer backbone but below T^* this mobility becomes 'frozen'. This interpretation is fully consistent with the concept

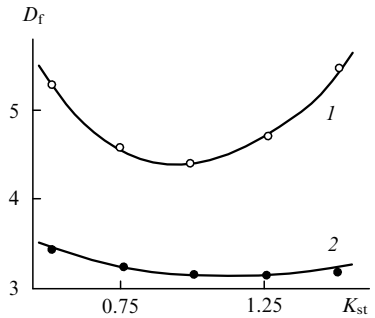


Figure 20. Dimensions of the regions of localisation of excess energy D_f *vs.* the curing agent : oligomer ratio K_{st} for EP-2 samples immediately after preparation (*1*) and after physical ageing (*2*).

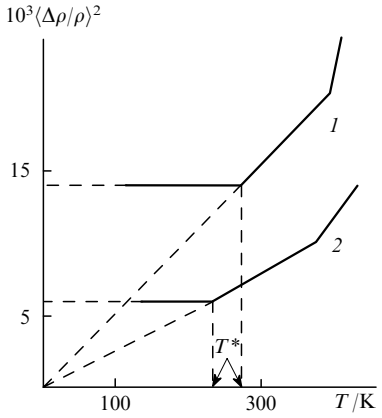


Figure 21. Temperature dependences of the density fluctuations $\langle\Delta\rho/\rho\rangle^2$ for poly(methyl methacrylate) (*1*) and poly(ethylene terephthalate) (*2*).[117]

of quasi-equilibrium state ($D = 1$). The nature of the temperature T^* has been considered in detail.[117]

Thus, the introduction of the concept of quasi-equilibrium state in polymers provides interpretation of some experimental facts. The application of the cluster model and fractal analysis makes it possible to specify the direction of the process of synthesis and to estimate its main characteristics.

4. Fluctuation free volume in polymers

The properties of polymers are mainly related to the molecular mobility and structure, which is determined by the degree of ordering of macromolecules.[118] Free volume, or, more precisely, one of its components, fluctuation free volume, is one of the parameters most suitable for phenomenological description of a structure.[119] As a rule, the fraction of the fluctuation free volume f_{fv} is estimated on the basis of polymer properties rather than from structure characteristics. Within the framework of the cluster model of the amorphous state of polymers,[74, 120, 121] it has been shown [57] that a microcavity of fluctuation free volume is formed upon detachment (dissociation) of a segment from a region of local order (cluster) and 'collapses' upon attachment of a segment to a cluster. If this mechanism is accepted, at least two aspects need to be considered. One aspect concerns the energy characteristics of the process. The cluster model for the structure of the amorphous state of polymers postulates the thermofluctuational character of local ordering, according to which the number of segments in clusters diminishes as the temperature increases;[122] this results in the formation of new microcavities of the fluctuation free volume (their nature has been considered in detail [123]) and in an increase in f_{fv}. It is evident that the energy of thermal fluctuations is of the order of kT; the energy of formation of a microcavity (ε_h) can be estimated from the equation

$$\varepsilon_h = kT_g \ln \frac{1}{f_{fv}}. \tag{54}$$

Since the maximum f_{fv} value expected in the vitreous state is 0.159 (according to the most 'rigorous' estimates [124]) and $T < T_g$, it is obvious that the energy of thermal fluctuations is insufficient for the formation of a microcavity.

The second point is determination of the f_{fv} value. This can be done by virtue of the following equation:

$$f_{fv} \simeq 0.017 \frac{1+\mu}{1-2\mu}. \tag{55}$$

For amorphous vitreous polymers, $f_{fv} \simeq 0.050-0.090$,[121] which is much greater than the value $f_{fv} \simeq 0.025 \pm 0.003$, which has been found in terms of the Williams – Landell – Ferry (WLF) concept and is generally accepted for most polymers.[118]

Evaluation of some polymer properties requires not only the integral characteristic f_{fv} but also the parameters of a separate

microcavity of fluctuation free volume, which is traditionally represented as a sphere with volume V_h.[119]

Recalling that the fractal dimension of the polymer structure is in the range $2 \leqslant d_f \leqslant 3$, it can be suggested that the fluctuation free volume as a structural unit also possesses fractal properties. Using relations (55) and (23), the dependence of f_{fv} on d_f has been elucidated [60]

$$f_{fv} \simeq 8.5 \times 10^{-3} \frac{d_f}{3 - d_f}. \quad (56)$$

If the above assumption is correct, the following general relation should hold:[125]

$$N_h \propto r_h^{D_{ffv}}, \quad (57)$$

where N_h is the number of microcavities, r_h is their characteristic size, and D_{ffv} is the fractal dimension of the fluctuation free volume.

As a first approximation, the r_h value can be expressed in terms of the microcavity volume as $V_h^{1/3}$, the volume being found from the equation

$$V_h = \frac{3(1-\mu)kT_g}{f_{fv}E}. \quad (58)$$

Although this approximation introduces some inaccuracy to the quantitative results, it does not deteriorate the generality of the conclusions.

The number of microcavities N_h is expressed as the ratio [119]

$$N_h = \frac{f_{fv}}{V_h}. \quad (59)$$

Figure 22 presents the variation of $\ln N_h$ as a function of $\ln V_h^{1/3}$ for specimens of three epoxy polymers, EP-1, EP-2, and aged EP-2, which is designated by EP-3. It can be seen that the plots are linear; this is a typical feature of fractal behaviour. The D_{ffv} values found from relation (57) for EP-1 and EP-2 were 5.9; that for EP-3 was 2.7.

It is clear that D_{ffv} calculated in this way are averaged values; nevertheless, they provide grounds for an important conclusion: in the general case, a microcavity of fluctuation free volume can be represented by a D_{ffv}-dimensional sphere, modelling by a three-dimensional sphere being a specific case. The D_{ffv} values are close to the corresponding dimensions D_f of the regions of localisation of excess energy, which are determined from Eqn (39). In addition, D_f is equal to the automodelling coefficient Λ_i and, hence, to C_∞. The fractal dimension D_{ffv} interpreted in this way is closely related to the characteristics of the polymer structure.

Now we consider the energy criterion for the formation of a microcavity with the volume V_h. For this purpose, we use the concept of free fracture of solids,[126] according to which a limited amount of potential energy with density A^* can be accumulated in a limited volume V and the formation of a new surface requires work equal to the product of the surface area S_n and the specific surface energy σ_n. In the case of free fracture,[127]

$$A^* V = \sigma_n S_n. \quad (60)$$

As applied to the formation of a microcavity with the volume $V = V_h$, relation (60) can be represented as follows:[87]

$$\frac{V}{S_n} = \frac{\sigma_n}{A^*}. \quad (61)$$

For a D_{ffv}-dimensional sphere, it can be written that [87]

$$\frac{V}{S_n} = \frac{r_h}{D_{ffv}}. \quad (62)$$

The σ_n value can be represented as follows:[119]

$$\sigma_n = \frac{\varepsilon_h}{2V_h^{2/3}}, \quad (63)$$

where ε_h is estimated from Eqn (54).

Finally, by determining A^* as the ratio

$$A^* = \frac{kT}{V_h}, \quad (64)$$

and using Eqns (61) and (63), we obtain

$$D_{ffv} = \frac{4\pi T}{T_g \ln(1/f_{fv})}. \quad (65)$$

Since ageing can be interpreted as a tendency towards thermodynamic equilibrium,[114] it is assumed that the condition $D_{ffv} = 3$ corresponds to a certain quasi-equilibrium state of the polymer. This allows one to draw several conclusions. First, an increase in temperature, all other factors being the same, implies an increase in D_f and, hence, enhancement of the thermodynamic nonequilibrium of the polymer as a system. It follows from Eqn (39) that an increase in D_f is accompanied by an increase in μ; this accounts for the well-known fact that the Poisson coefficient of polymers increases with temperature.[74, 127, 128] Second, an increase in μ implies a decrease in the degree of local ordering of amorphous polymers,[70, 129] which is manifested as a decrease in the density of the cluster network of entanglements V_{en}. In other words, an increase in V_{en} reflects the trend of a polymer towads thermodynamic equilibrium.[114] Third, in the case where $D_{ffv} = 3$, one can calculate the relative portion of the 'quasi-equilibrium' free volume (f'_{fv}); for the epoxy polymers in question, it falls in the range $\sim 0.028 - 0.042$, which is rather close to the f_{fv} value in the WLF equation mentioned above. Thus, the estimation of f_{fv} using Eqn (55) is correct and the considerable magnitudes of f_{fv} reflect a relatively high degree of thermodynamic nonequilibrium in epoxy polymers.

Let us consider the general statements of the concept of fluctuation free volume in relation to cross-linked systems. Figure 23 *a* illustrates the relationship between the fractal dimensions of the regions of localisation of excess energy D_f [see Eqn (39)] and the fluctuation free volume D_{ffv} [see Eqn (65)]. It can be seen that these two values are fairly close to each other.‡ Thus, the f_{fv} value can actually be used to characterise the polymer structure.

The formation of a microcavity with the volume V_h requires local critical deformation ε_c[130]

$$\varepsilon_c = \frac{1}{3} \frac{\ln(1/f_{fv})}{3\gamma}, \quad (66)$$

where γ is the Grüneisen parameter, characterising the anharmonicity of the intermolecular bonds in a polymer and the factor 3 was introduced under the assumption that a microcavity is three-dimensional. In view of this fact, this factor should be replaced by D_{ffv} and thus Eqn (66) assumes the form

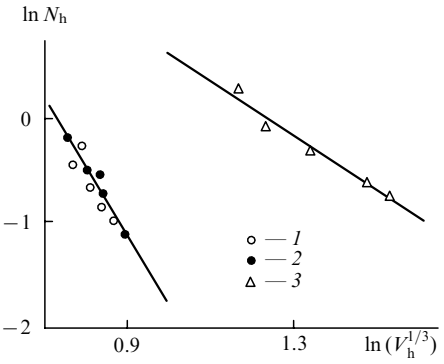


Figure 22. Number of microcavities of fluctuation free volume *vs*. their size for EP-1 (*1*), EP-2 (*2*) and EP-3 (*3*).

‡ Some discrepancy is due to the fluctuation nature of free volume.

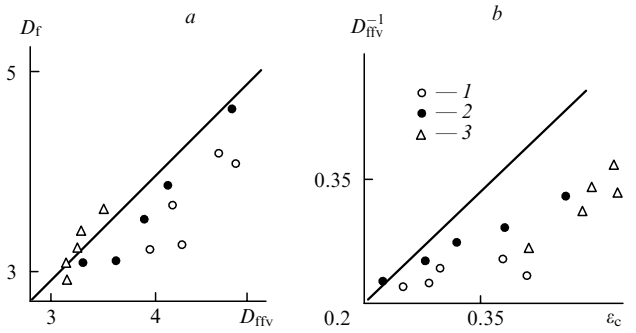


Figure 23. Relationships between the fractal dimensions of the regions of localisation of excess energy D_f and the fluctuation free volume D_{ffv} (*a*) and between the dimension of the fluctuation free volume and the critical deformation in the formation of microcavities ε_c (*b*) for EP-1 (*1*), EP-2 (*2*) and EP-3 (*3*).

$$\varepsilon_c = \frac{\ln(1/f_{fv})}{3\gamma D_{ffv}}. \tag{67}$$

Thus, the more pronounced the fractality of the fluctuation free volume (the greater D_{ffv}), the smaller ε_c and the easier the formation of the microcavity. This fact is reflected in the dependence of ε_c on D_{ffv}^{-1} (Fig. 23 *b*). The γ value was found from the relation [130]

$$\gamma \simeq 0.74\frac{1+\mu}{1-2\mu}. \tag{68}$$

It is noteworthy that the Grüneisen parameter varies in parallel with D_{ffv} and is related to the dimension of the fluctuation free volume by the following simple relation:

$$\gamma \simeq D_{ffv} - 1. \tag{69}$$

In other words, the Grüneisen parameter is also a fractal characteristic; for quasi-equilibrium conditions, $\gamma = 2$. The values $\gamma > 2$ mean an enhanced nonequilibrium character of the system.[131]

Figure 24 shows the dependence of γ on D_{ffv} and the dependence of V_h on K_{st} for three epoxy polymers. The V_h values for EP-1 and EP-2 vary from 0.97 to 7.31 nm^3 but those for EP-3 are greater and lie in the range of 5.45 – 10.1 nm^3. In terms of the free fracture concept, this implies that the formation of a microcavity in a system the state of which is close to quasi-equilibrium requires more thermal fluctuations with the energy kT than that in nonequilibrium systems (EP-1 or EP-2). The same requirement is valid for each particular composition, which is confirmed by the presence of a maximum on the dependence of V_h on K_{st} at $K_{st} = 1$. The degree of equilibration can be estimated as the difference

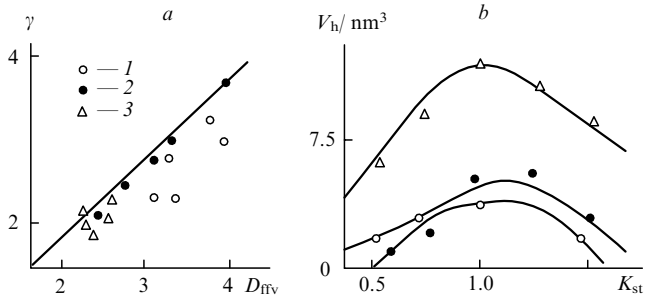


Figure 24. Relationship between the Grüneisen parameter γ and the dimension of the fluctuation free volume D_{ffv} (*a*) and the dependence of V_h on K_{st} (*b*) for EP-1 (*1*), EP-2 (*2*) and EP-3 (*3*).

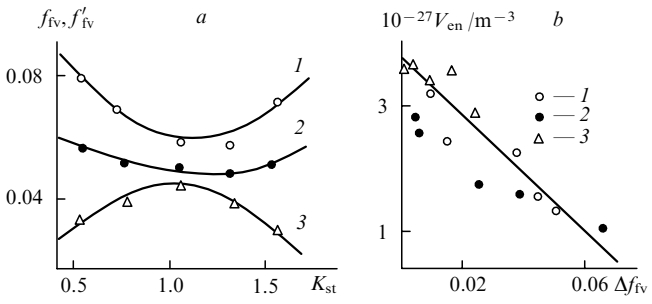


Figure 25. Variation of f_{fv} *vs.* K_{st} (*a*) and of the density of the cluster network of entanglements V_{en} *vs.* Δf_{fv} (*b*) for epoxy polymers. (*a*): (*1*) EP-1, $f'_{fv}(K_{st})$; (*2*) EP-1, $f_{fv}(K_{st})$; (*3*) EP-3, $f_{fv}(K_{st})$; (*b*): (*1*) EP-1, (*2*) EP-2, (*3*) EP-3.

$$\Delta f_{fv} = f_{fv} - f'_{fv}. \tag{70}$$

The meaning of this estimate becomes evident if one compares the $f_{fv}(K_{st})$ and $f'_{fv}(K_{st})$ plots for EP-1 and EP-3 (Fig. 25 *a*). As noted above, samples with $K_{st} = 1$ are closest to the quasi-equilibrium state. The aged EP-3 samples at $K_{st} = 1$ have already reached this state and further ageing does not change the structure. The samples with $K_{st} \leqslant 0.50$ and those with $K_{st} \geqslant 1.50$ possess the lowest stability during physical ageing, which is displayed as the corresponding change in their properties. The decrease in the elastic modulus during ageing of EP-1 amounted to 1.7 GPa for $K_{st} = 1.50$ and 1.1 GPa for $K_{st} = 1.0$. Thus, by comparing the $f_{fv}(K_{st})$ and $f'_{fv}(K_{st})$ plots, one can demonstrate the degree of thermodynamic nonequilibrium of cross-linked systems and predict the possible changes in their structure and properties during physical ageing.

The closeness of a polymer to the equilibrium state can be characterised by the degree of ordering. Using the cluster model, this trend can be quantitatively described fairly easily in terms of the parameters V_{en} or φ_{cl}.[57,132] The dependence of V_{en} on Δf_{fv} (Fig. 25 *b*) shows that the degree of local ordering can serve as an indication of the thermodynamic nonequilibrium of the polymer structure. Extrapolation of the straight line $V_{en}(\Delta f_{fv})$ to $\Delta f_{fv} = 0$ gives $V_{en} \simeq 3.8 \times 10^{27}$ m^{-3}, which is about 1.5 times lower than the maximum V_{en} value found as the ratio of the total length of the macromolecule per unit volume of the polymer to the length of the statistical segment.[133] This discrepancy stipulates the legitimacy of applying the term 'quasi-equilibrium state' to the polymer structure with $\Delta f_{fv} = 0$. It is clear that an equilibrium state implies that all macromolecules are packed in the regions of local ordering. It has been shown [70] that the condition $\Delta f_{fv} = 0$ cannot be attained for the epoxy polymers in question even for the maximum possible V_{en} value. Yet another important feature of the quasi-equilibrium state is temperature dependence of parameters, in particular, f_{fv} [see Eqn (65)]. When $V_{en} = 0$, the straight line $V_{en}(\Delta f_{fv})$ is extrapolated to $\Delta f_{fv} \simeq 0.077$, which also has a definite physical meaning. For $f'_{fv} = 0.035$ (see Fig. 25 *a*) and $\Delta f_{fv} \simeq 0.077$, the f_{fv} value is equal to 0.112, which is close to the fluctuation free volume at T_g.[118,119] Thus, the destruction of clusters can be identified with glass transition of cross-linked polymers.

Thus, the above results point to the fractality of the fluctuation free volume in cross-linked polymers. In this connection, one important fact should be noted, which has not received adequate attention before. In accordance with Eqn (58), V_h decreases with an increase in f_{fv}. For pores with sizes of the order of several nanometers, it has been shown [134,135] that

$$-\frac{dV}{d\rho} \propto \rho^{2-D'}, \tag{71}$$

where V is the total pore volume, ρ is the average pore radius, and D' is the fractal dimension of the structure of a porous material.

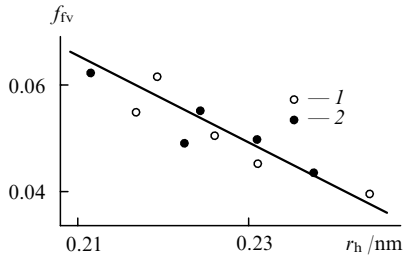


Figure 26. Relative fluctuation free volume f_{fv} *vs.* radius of the free volume microcavities r_h for EP-1 (*1*) and EP-2 (*2*).

According to different estimates, the linear sizes of microcavities of free volume r_h vary from 0.2 to 1.5 nm.[136–142] If we assume that $V_h = f_{fv}$ and $r = r_h$, for Eqn (71) to have a physical meaning, it is evidently required that the slope of the $f_{fv}(r_h)$ plot be negative. The calculated D' values for EP-1 and EP-2 vary from 4.78 to 5.31, which is consistent with the above estimates of D_{ffv} and D_f. Figure 26 presents the dependence of f_{fv} on r_h, which is linear and has a negative slope. Figure 27 illustrates the relationship between D_f and D'. It can be seen that D' values are regularly greater than D_f but both values vary according to the same pattern and the deviations do not exceed 25%. This also attests to the fractality of the free volume the dimension of which reflects the extent of 'pumping' of energy into the polymer and does not coincide with the corresponding dimension of the polymer structure.

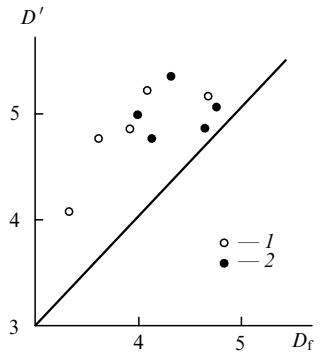


Figure 27. Relationship between the fractal dimensions D' and D_f calculated from Eqns (71) and (39), respectively, for EP-1 (*1*) and EP-2 (*2*).

Let us consider the influence of the 'pumping' of energy (mechanical or thermal) on the formation of free volume in epoxy polymers. Within the framework of the Frenkel' kinetic theory,[115] the radius of a microcavity of free volume r_h depends on the surface tension σ

$$r_h^2 = \frac{\varepsilon_h}{4\pi\sigma}. \qquad (72)$$

Equation (72), which is an analogue of relation (63), permits calculation of σ provided that r_h and ε_h are known. The dependence of the σ values thus found on D_f for EP-1 and EP-2 is plotted in Fig. 28. An increase in D_f (enhancement of energy pumping from the outside) results in a decrease in σ, which facilitates the formation of a microcavity of the fluctuation free volume. Note that for $D_f = 7.7$, the σ value becomes equal to zero. This is unlikely from the physical viewpoint; nevertheless, it is evident that σ sharply diminishes on moving towards $D_f \simeq 7.7$. This D_f value is matched by $\mu \simeq 0.425$ [according to Eqn (39)], which corresponds to the mechanical [74] and thermal [143] glass transition process. It has been shown experimentally that V_h sharply increases (and, hence, σ decreases) [136] and the yield point increases[144] at T_g.

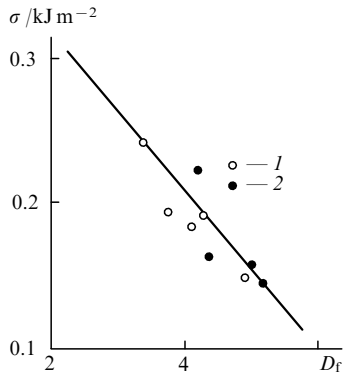


Figure 28. Surface tension *vs.* fractal dimension of the regions of localisation of excess energy for EP-1 (*1*) and EP-2 (*2*).

The variation of f_{fv} as a function of D_f is presented in Fig. 29. The straight line was drawn with the assumption that for $\mu = 0$ (which corresponds to close packing of an amorphous polymer [129]), $D_f = 2$ and $f_{fv} = 0$, whereas for the maximum possible f_{fv} value at T_g [$f_{fv}^t \simeq 0.159$ (see Ref. 124)], $\mu \simeq 0.44$ and $D_f^t \simeq 9.3$. The f_{fv} values found using relation (55) for EP-1 and EP-2 correspond to the proposed model. Thus, 'pumping' of energy into a polymer increases the dimensions of the regions in which it is localised and increases the fluctuation free volume.

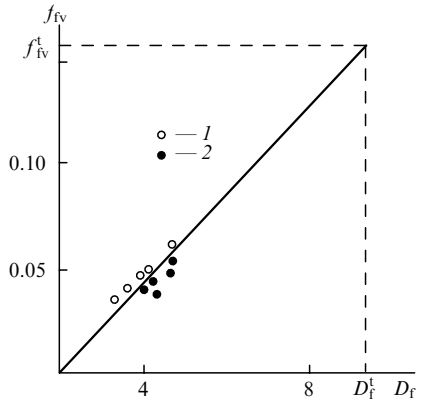


Figure 29. Relationship between the relative fluctuation free volume f_{fv} and the dimension of the regions of localisation of excess energy D_f. The points correspond to the calculation of f_{fv} from Eqn (55) for EP-1 (*1*) and EP-2 (*2*). The explanations are in the text.[153]

Thus, the fluctuation free volume in vitreous polymers has a fractal structure; therefore, the microcavities that constitute the free volume can be modelled by a D_{ffv}-dimensional sphere. The sizes of microcavities are controlled by the volume in which the energy of thermal fluctuations needed for their formation is accumulated. The absolute magnitudes of f_{fv} can characterise the thermodynamic nonequilibrium of the polymer structure. For quasi-equilibrium structures, it is assumed to be equal to f_{fv} in the known WLF equation. The dimension of the free volume regions (which coincides with the corresponding dimension of the regions of localisation of energy pumped from the outside) reflects the extent of energetic excitation of the polymer structure.

5. Fractal characteristics of polymers in time-dependent processes

Polymers obey the principle of temperature–time superposition,[145, 146] according to which structural (including fractal) characteristics of polymers are functions of the time scale of testing. In this connection, we shall consider the influence of the

time factor on the fractal characteristics in processes typical of polymers such as thermal ageing or relaxation.

The dependences of the dielectric loss tangent ($\tan\delta$) on the Hausdorff dimension for several copolymers have different slopes at measurement frequencies of 1 and 10 kHz. This hampers correct prediction of $\tan\delta$. This difference can be easily explained in terms of the cluster model. The φ_{cl} value is a parameter of the order of the polymer structure;[60] due to the thermodynamic nonequilibrium of the structure, it is also a function of the time scale t. In the general case, the time-dependent order parameter $\varphi_{cl}(t)$ is determined as follows:[147]

$$\varphi_{cl}(t) = \varphi_{cl}^{0} \exp\left(-\frac{t}{\tau_0}\right), \tag{73}$$

where φ_{cl}^{0} is the φ_{cl} value at very large t and τ_0 is the relaxation time under normal conditions.

If the time scale of the experiment is expressed in terms of π/ω (ω is the frequency of measurements) and the relaxation time is assumed to be $\tau \simeq 10$ ms, the φ_{cl} value can be estimated as a function of frequency and, hence, different D values for frequencies of 1 and 10 kHz can be obtained. An increase in D (decrease in t) results in higher φ_{cl} [according to Eqn (73)] and in lower D.[14] Therefore, the dependence of $\tan\delta$ on D is described by one straight line for both frequencies mentioned above.[26] Thus clusters can be generally defined as regions in which relaxation processes are impossible.

Physical ageing of amorphous vitreous polymers consists in the variation of the structure and properties with time, which reflects the thermodynamically nonequilibrium nature of these polymers.[114] At relatively low temperatures (about room temperature), this process is fairly slow; it takes several years for substantial changes in the properties to occur.[94, 148] Therefore, forecasting of these phenomena should be performed with allowance for both spatial and temporal disorder of systems. The spatial non-uniformity of the structure of amorphous vitreous polymers accounts for the rather broad range of the rates of relaxation processes. Spatial disorder results in temporal disorder. The variation of the properties and structure of polymers during ageing can be described quantitatively within the framework of fractal analysis.

Study of the reaction dynamics in disordered systems has shown that for most reactions at long times, subordination expressed by the following general relation is obeyed:[149]

$$\Phi \propto t^{\alpha\gamma}, \tag{74}$$

where Φ is an arbitrary function dependent on time t and α and γ are coefficients taking into account the spatial and temporal disorder.

As applied to physical ageing, the variation of structure with time can be described, on the basis of general relation (74), in the following way:[150]

$$V_{cl} = C V_{cl}^{0} t^{\alpha\gamma}, \tag{75}$$

where V_{cl} and V_{cl}^{0} are the densities of the cluster network of entanglements in the aged and initial polymers, respectively; C is a proportionality coefficient. The index α can be defined in terms of fractal analysis as the difference $d_f - 2$, where d_f is the fractal dimension of the structure of the initial epoxy polymer, with allowance for the following considerations: the $2 < d_f \leqslant 3$ range characterises the degree of disorder of the polymer structure;[151] most information on this point is carried by the fractional part of d_f: the greater the magnitude of d_f, the lower the local order and, hence, the higher the spatial disorder of the system.[152]

The quasi-equilibrium state of polymers is characterised by $d_f \simeq 2.5$. This value corresponds to a fully relaxed polymer with a narrow size distribution of free volume cavities[153] and, hence, to the least temporal disorder, characterised by a spectrum of relaxation times. Therefore, the following approximation has been used:[150]

$$\gamma = d_f - 2.5. \tag{76}$$

Thus, Eqn (75) can be finally written in the form

$$V_{cl} = V_{cl}^{0} C t^{(d_f-2)(d_f-2.5)}, \tag{77}$$

where the coefficient C determined empirically is equal to ~ 0.14 and the time of ageing is expressed in seconds.

Figure 30 shows the dependences of φ_{cl} on K_{st} for the initial (EP-2) and aged (EP-3) epoxy polymers. In the case of EP-3, the φ_{cl} values determined experimentally and calculated using Eqn (77) are given. It can be seen that the experimental and calculated values are in good agreement. The maximum deviations for K_{st} equal to 0.50 and 1.50 do not exceed $\sim 25\%$. It is assumed[150] that the main reason for the inaccuracy is the high power dependence of V_{cl} on d_f in Eqn (77).

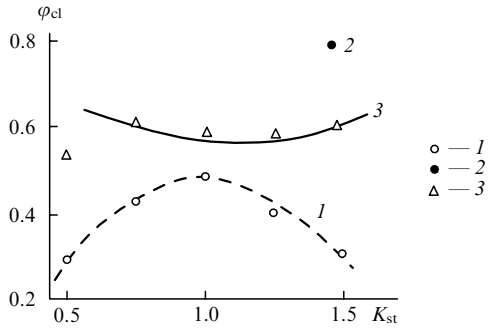


Figure 30. Relative portion of clusters φ_{cl} *vs.* the curing agent : oligomer ratio K_{st} for EP-2 (*1*) and EP-3 (*2*, *3*);
(*1*, *2*) experimental data, (*3*) calculation using Eqn (77).[150]

Yet another important aspect of physical ageing is also associated with the dependence of φ_{cl} on K_{st} (see Fig. 30). The ageing rate expressed as the difference between the φ_{cl} values for EP-2 and EP-3 varies substantially for different K_{st} (and, hence, for different chemical cross-linking densities ν_s). The minimum ageing rate is observed for a system with $K_{st} = 1.0$;[152] deviations from this value towards both greater and lower values result in an increase in the ageing rate.[101] This is due to an increase in both α and γ [see Eqn (77)] or, in other words, to an increase in the fractal dimension of the structure d_f.

Parameters which vary during physical ageing include not only supermolecular structure characteristics (d_f and D_f) but also the statistical chain flexibility index C_∞. Using Eqns (39) and (41), it can be written that

$$A_i = C_\infty = D_f = 2\,\frac{1-\mu}{1-2\mu}. \tag{78}$$

The physical ageing results ultimately in the formation of similar structures for all the epoxy polymers considered, irrespective of the density of chemical cross-linking points (ν_s varies by approximately an order of magnitude).[154] Naturally, this structure equalisation also determines substantial convegence of the properties of EP-2 and EP-3.[94]

From the practical viewpoint, it is important to predict the properties of polymers during physical ageing. A procedure suitable for this purpose has been reported.[150] This procedure is based on Eqn (77). Knowing the V_{cl} and C_∞ values, one can estimate D_f and calculate E.[155] Then the yield point σ_p[142, 148] and some characteristics of polymers[64, 156] can be determined.

In recent years, considerable attention has been paid to investigation of the relaxation processes in complex condensed systems. An example of this type of system is amorphous-crystalline polyethylene, the structure of which under normal conditions consists of crystalline regions, regions of local ordering and a devitrified loosely packed matrix.[157, 158] The interest in these

studies is caused by the experimental fact that the correlation functions for many different systems vary in accordance with the same exponential dependence

$$\varphi(t) = \exp\left[-\left(\frac{t}{\tau}\right)^{\beta}\right], \quad 0 < \beta < 1. \tag{79}$$

The parameters β and τ depend both on the material and on the environmental conditions, for example, temperature.

The law described by Eqn (79) was first proposed by Kohlrausch and has later been used by Williams and Watts to describe the dielectric relaxation in polymers (M Schlesinger, J Klafter, see Ref. 149, p. 553). The main difficulty in the case of polymers is to identify the parameters of Eqn (79) in terms of characteristics describing the polymer structure. This identification has been performed within the framework of fractal analysis.[39]

In the impact testing of polymers, the elastic modulus decreases with an increase in the time scale of testing (in the case of brittle fracture, this is time to fracture t') and can be described by the empirical relation [159, 160]

$$E = E_0(t')^{-m}, \tag{80}$$

where E_0 is the 'unity' modulus, *i.e.* the E value for $t' = 1$ on the time scale chosen, and m is an empirical index characterising the degree of completeness of relaxation processes.

Figure 31 shows the variation of E as a function of t' corresponding to Eqn (80) for high-density polyethylene samples with different lengths of a sharp notch (an increase in the length decreases t') at a testing temperature of 293 K. The slope of the straight line can be used to estimate the index m, while extrapolation of the plot to $t' = 1$ gives the E_0 value. It should be noted that at certain t' values (for example, τ), the variation of $\ln E$ *vs.* $\ln(1/t')$ has a break — at $t' < \tau$ the elastic modulus increases faster than at $t' > \tau$, which reflects an increase in m. This finding is related to the extent of completeness of relaxation processes: at $t' > \tau$ this extent is high and, correspondingly, the increase in E is insignificant.

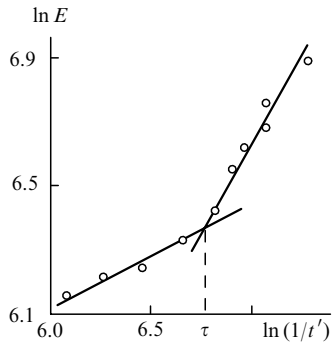


Figure 31. Elastic modulus E *vs.* time to fracture t' [see Eqn (80)] for high-density polyethylene samples with a sharp notch; $\tau = \tau_0$ is relaxation time.[153]

The difficulty in describing the variation of E according to Eqn (80) is due to the presence of two empirical constants (E_0 and m), which, moreover, can change discretely. Therefore, an alternative approach based on the use of the Kohlrausch equation (79) has been chosen.[153] To describe E, this equation should be written in the form

$$E = E'_0 \exp\left[-\left(\frac{t'}{\tau_0}\right)^{\beta}\right], \quad 0 < \beta < 1, \tag{81}$$

where E'_0 is a constant.

Let us consider the physical meaning of the parameters appearing in Eqn (81). It is evident that the τ value can be taken as τ_0 (see Fig. 31). The constant E'_0 determines the maximum elastic modulus E_{max} which can be attained for a given polymer without relaxation. The range of variation of this parameter for very high testing frequencies (several megahertz) was found [161] to be 1.1–2.6 GPa for high- and low-density polyethylene. Finally, the index β, characterising the width of the relaxation spectrum (spatial disorder of the system), can be associated with the fractional part of d_f, *i.e.* it is taken to be equal to $d_f - 2$. Note that both β and $d_f - 2$ vary over the same limits. Thus, the final form of the Kohlrausch equation for determining the elastic modulus of polymers under high-speed loading (brittle fracture) can be written as follows [153]

$$E = E_{max} \exp\left[-\left(\frac{t'}{\tau}\right)^{d_f - 2}\right], \quad 0 < (d_f - 2) < 1. \tag{82}$$

Figure 32 shows the dependences of the E values, both experimental and calculated from Eqn (82), on the sharp notch length l for high-density polyethylene samples at different temperatures. Good agreement between the theoretical and experimental results is obvious.

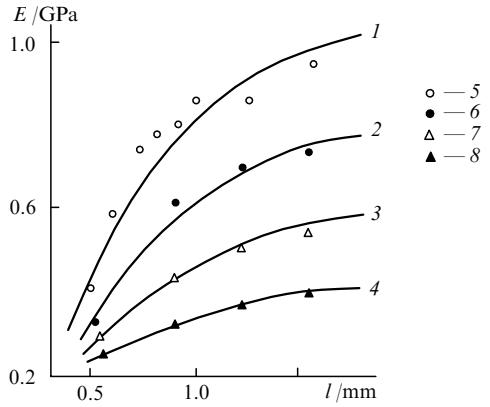


Figure 32. Experimental (*1–4*) and calculated [Eqn (82)] (*5–8*) elastic moduli E *vs.* length of the sharp notch l for high-density polyethylene at testing temperatures of 293 (*1*, *5*), 313 (*2*, *6*), 333 (*3*, *7*) and 353 K (*4*, *8*).[153]

Thus, methods of fractal analysis in combination with the cluster model of the structure of amorphous polymers provide a quantitative description of time-dependent processes. The fact that the fractal dimension of the structure d_f takes into account both the spatial and temporal disorder accounts for the simplicity of the resulting equations.[150]

III. Modelling of the structure and properties of polymers

1. Modelling in terms of the percolation theory

Percolation models are widely used to describe critical phenomena [162] including those in polymers.[162–166] Percolation clusters are homogeneous fractals when $x \neq x_c$ (x is the current coordinate, x_c is the coordinate of the percolation transition). For example, the structure of vitreous polymers is a fractal when $T \neq T_g$ or, with allowance for the foregoing, when $T < T_g$.

It should be borne in mind that the fractal properties of the polymer structure are due to the presence of the cluster structure or, more precisely, of 'frozen' ordering. However, as has already been mentioned, the magnitude of the fractal dimension of the structure d_f for amorphous polymers is debated, the overall range being $2 \leqslant d_f \leqslant 3$.[125] Thus on the basis of theoretical statements of Alexander and Orbach,[43] it has been concluded [167] that for an ideal disordered linear polymer, d_f is equal to 2, while for real amorphous polymers, this value is 2.0–2.2. Let us make several rather simple estimates of d_f for epoxy polymers EP-1 and EP-2. For a percolation system, the following relation holds:[162]

$$d_f = d - \frac{\beta}{\nu}, \quad (83)$$

where d is the dimension of the Euclidean space in which the fractal is inserted and β and ν are critical indices of a percolation system related to each other as

$$d\nu = 2\beta + \gamma_c, \quad (84)$$

where γ_c is also a critical index of the percolation system. The parameters calculated from Eqn (83) are listed in Table 2.

Table 2. Parameters of percolation systems for epoxy polymers.

Parameter	Experiment		Calculation using Eqn (83)
	EP-1	EP-2	
ν	0.67	1.15	0.88
β / ν	0.537	0.504	0.455
d_f	2.46	2.50	2.545

The evaluation of the index ν for EP-1 and EP-2 for $d = 3$ using Eqn (84) and the β and γ_c values determined previously gives 0.67 and 1.15, respectively, which is consistent with the theoretical value $\nu = 0.88$ (see Table 2).

The d_f values for epoxy polymers estimated using Eqn (23) fall in the range from 2.56 to 2.73, which is in good agreement with the estimates made in this review but is substantially greater than has been assumed previously.[43, 167]

The following ratio for percolation clusters has been reported:

$$d_{super} = \frac{d_f}{d_s}, \quad (85)$$

where $d_{super} > 1$ is so-called superlocalised index.

Using the d_{super} and d_s values found experimentally for epoxy polymers based on bisphenol A,[167, 168] we calculated d_f, which proved to be 2.55. This value is close to the above estimates. Note that the application of Eqn (85) to the calculation of d_{super} of epoxy polymers became possible owing to the representation of their structure as a percolation system.

The d_f value can also be estimated without experimental d_s but using only the index d_{super}. For example, the random walk dimension d_w can be represented, with allowance for Eqn (85), in the following form:

$$d_w = 2\, d_{super}. \quad (86)$$

The d_f values for the epoxy polymer at $d_{super} = 1.85$ [167] amounted to 2.47 and 2.70 in accordance with the Alexander–Orbach and Aharoni–Stauffer hypotheses,[48] respectively. These values are close to the estimates made using Eqn (23).[167]

The fractal dimension is determined by the disorder which is generated by deterministic chaos. This statement can be expressed in the analytical form [169]

$$d_f = \frac{S}{\lambda}, \quad (87)$$

where S is the entropy of the system, λ is the Lyapunov index.

The entropy change ΔS in a chaotic process can be determined using the following simple formula:[170, 171]

$$\Delta S \simeq 3k f_{fv} \ln f_{fv}, \quad (88)$$

where f_{fv} is determined from Eqn (55) and k is the Boltzmann constant.

Figure 33 shows the variation of d_f [calculated in terms of Eqn (23)] as a function of ΔS [calculated using Eqn (88)] for the epoxy polymers under consideration. This plot has some interesting features. First, extrapolation of the $d_f(\Delta S)$ straight line to $\Delta S = 0$ yields the value $d_f = 2$. Relation (88) indicates that the condition $\Delta S = 0$ is matched by $f_{fv} = 0$. This implies close packing

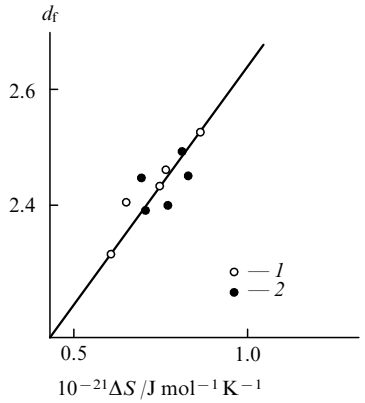


Figure 33. Fractal dimension d_f of the structure *vs*. entropy for EP-1 (*1*) and EP-2 (*2*).[170]

of the structure of epoxy polymers. In other words, the value $d_f = 2$ is attained for an amorphous polymer in the case of close packing rather than in the case of ideal disorder, as has been suggested in a previous publication.[167] Second, $d_f = 3$ is attained at a ΔS value corresponding to $f_{fv} \simeq 0.157$. This is known to be the greatest theoretical value relative to the free volume at T_g.[124] This means that $d_f = 3$ corresponds to the devitrified state of the polymer, *i.e*. to destruction of the local 'frozen' order. This fact confirms the relationship between local order and fractality of amorphous polymers. Third, in accordance with relation (87), the linear dependence of d_f on ΔS means that λ = const. Thus, the chaotic component of the dynamics of structure formation is the same for the epoxy polymers considered.[172]

Thus, the structure formed in epoxy polymers at the glass transition temperatutre T_g is a percolation cluster, which is described adequately in terms of the cluster model.[57, 173] Therefore, it can be assumed that glass transition of a polymer is a phase transition and φ_{cl} is an order parameter. In addition, this fact can serve as evidence confirming fractality of the structure of network polymers (for $T < T_g$) in the range of length scales of ~ 0.3–5.0 nm. The fractal dimension of the structure of epoxy polymers is much greater than it has been believed previously (see, for example, Ref. 60); it is determined by the disorder generated by deterministic chaos. The loss of fractality by the epoxy polymer structure, *i.e*. the situation when $d_f = d$ is attained at the glass transition temperature.

It is worth noting that the model of percolation cluster proposed by Kozlov *et al*.[166, 170] is similar in essence to the concept of critical thermal transition.[19] According to this concept, the portion of system elements belonging to the greatest cluster is proportional to the order parameter, which varies near the critical temperature T^* as ε^β, where $\varepsilon = (T - T^*)/T^*$.

2. The model of diffusion-limited aggregation

The general description of the models of irreversible aggregation has been reported in several publications.[12, 162, 174] Here we shall consider particular aspects of using the model of diffusion-limited aggregation (DLA) for describing the structure of amorphous polymers. Note that the computer simulation procedures, widely used for this purpose, should be made more specific. If the cluster model of the structure of amorphous polymers [173–175] can be described as the Witten–Sander (WS) cluster, this means that the model and the WS cluster belong to the same class of universality.

There exist numerous reasons for representing the structure of an amorphous polymer as WS clusters and for assigning them to one class of universality. These reasons have been considered in detail;[60] here we mention only three most important ones.[176] The first reason is that the aggregation mechanism belongs to one class of universality; for WS clusters, this is attachment of separate particles to the growing clusters (aggregation of the particle–

cluster type). In terms of the cluster model, this mechanism is attachment of a statistical segment to a region of local order; this event is equivalent to the 'collapse' of a microcavity of the fluctuation free volume.[57, 121] The second reason follows from the first one: due to the identical aggregation mechanisms, the structures of amorphous polymers and the WS clusters have the same scaling indices, namely, the dimensions d_f (see Refs 170 and 171) and D (see Ref. 172), respectively. The third reason is as follows. It is known[44] that during the synthesis of polymers, the class of universality changes in the gelation point, namely, the cluster–cluster mechanism is replaced by the particle–cluster mechanism; the latter affords WS clusters.

The model representation (in terms of the DLA model) made it possible to describe the structures of EP-1 and EP-2; this was done using the same scaling index, namely, the dimension d_f.[175] It should be mentioned that the word 'cluster' is interpreted in different ways in the cluster model[177] and in the WS cluster model. In terms of the latter, the term 'cluster' denotes both the region of local ordering and the chains protruding from it, while in the former case, only statistical segments incorporated in the region of local ordering are meant. It is evident that the structure of a polymer sample cannot be regarded as a single WS cluster. Therefore, by analogy with Belousov *et al.*,[177] who proposed a modified variant of the WS model, we represent the structure of epoxy polymers by a set of WS clusters, the size of each cluster ranging from l_{st} to R_{cl}. Therefore, the model of multiple growth sites is the most plausible modification of the WS model. According to the WS model, the growth of a WS cluster takes place on a large number of seeds, the cluster size R_{cl} being related to the concentration of free diffusing particles N in the following way:

$$N \simeq R_{cl}^{D-d}. \tag{89}$$

Only those statistical segments that are located in the loosely packed matrix are able to join the region of local ordering. An increase in the degree of local ordering decreases the temperature; for R_{cl} = const, this means a decrease in the difference $D-d$ or a decrease in D. The N value was taken to be equal to the product of the number of particles (statistical segments) per unit volume and the proportion of the loosely packed matrix. Figure 34 shows the plots for the variation of the fractal dimensions of the epoxy polymer structures[156] and of the WS cluster, calculated using relation (89), *vs.* the curing agent : oligomer ratio. One can notice good correspondence between d_f and D.[175]

Thus, a modified version of the particle–cluster aggregation model[178] allows the structures of network polymers to be described in terms of D. This stipulates the assignment of the structure of network polymers to the given class of universality and, hence, description of its properties by relations developed for this class of universality.[175]

Description of the local ordering of the structure of amorphous polymers (in relation to polycarbonate and high-density polyethylene) in terms of the WS model has been reported.[176] The following equation characterises the variation of the density of the WS cluster ρ_{WS} as a function of its radius R_{WS} and the dimension D:[179]

$$\rho_{WS} = \rho\left(\frac{R_{WS}}{a}\right)^{D-d}, \tag{90}$$

where ρ is the density of the material of the WS cluster in the state of close packing, a is the lower boundary of the fractal behaviour of the WS cluster, which can be identified with the length of an elementary unit in the polymer chain.

A WS cluster obeys the relations $D < d$ and $\rho_{WS} < \rho$, which determine the condition $a < R_{WS}$. Replacement of the signs in the first two inequalities by equality signs implies transition of the cluster to another class of universality, for example, transition to the Eden cluster.[87] Meanwhile, since $\rho_{WS} \neq 0$ and $\rho \neq 0$, a cannot be equal to zero. Thus, a compact region ($D \simeq d$) with size a, identified as a region of local ordering for the structure of an amorphous polymer, always exists in the centre of the WS cluster. This statement is a necessary condition for the existence of the WS cluster.[180] Two remarks on this point are pertinent.

First, the cause for the appearance of the compact region at initial stages of formation of a WS cluster can be easily understood. Indeed, the fractal nature of the WS cluster is determined by the shielding effect of its 'branches', which prevent the access of particles into the inner regions of the cluster.[180, 181] However, in initial stages of the growth, these 'branches' are poorly developed and the shielding effect is low. Second, the polymer structure, as any real (physical) fractal, possesses fractal properties only in a particular range of length scales.[87] It has been shown experimentally[167, 182] that this range for polymers is from several Ångstrom to several tens of Ångstrom. This implies the presence of a density gradient in the polymer in this range of length scales, which, in turn, means alternation of blobs and rarefied sections in the material.[183] The cluster model[173, 177] satisfies this condition, whereas, for example, the 'felt' model of the polymer structure proposed by Flory[113] cannot account for the experimentally observed fractal properties.[167, 182, 183]

Thus, interpretation of the structure of an amorphous polymer as a WS cluster (more precisely, as a set of these clusters) assumes necessarily the existence of regions of local order. This has been confirmed[176] by comparing the a values calculated from Eqn (90) and the size of the region of local order r_{cl} (Fig. 35). The r_{cl} value can be found from the following equation (under the assumption of close packing):[184]

$$r_{cl} = \left(\frac{n_{cl}S}{\pi\eta}\right)^{1/2}, \tag{91}$$

where n_{cl} is the number of statistical segments in the cluster, η is the density of packing of the element, equal to 0.74.[184]

Figure 36 shows the variations of the size of the regions of local order r_{cl} in the cluster model[173] and the compact regions a in the WS model *vs.* testing temperature for polycarbonate and high-density polyethylene. In studies by Kozlov *et al.*,[176, 185] the density of the loosely packed polymer matrix, which coincides with the density of the polymer above the glass transition (melting) temperature, was taken as ρ_{WS} and the density of the crystalline

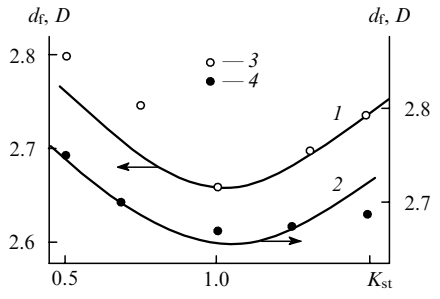


Figure 34. Fractal dimensions of the structure d_f (*1*, *2*) and of the WS clusters D (*3*, *4*) *vs.* the curing agent : oligomer ratio K_{st} for EP-1 (*1*, *3*) and EP-2 (*2*, *4*).[156]

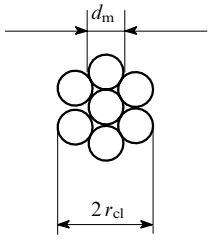


Figure 35. Cross-section of the region of local order incorporating seven statistical segments (d_m is the diameter of the polymer macromolecule).[175]

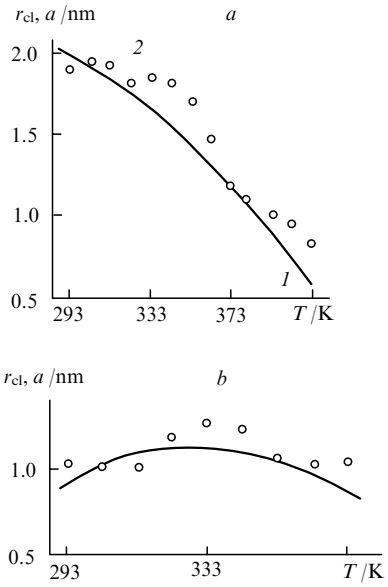


Figure 36. Size of the regions of local ordering r_{cl} (curve) in the cluster model and size of the compact regions a (dots) in the WS model *vs.* temperature for polycarbonate (*a*) and high-density polyethylene (*b*).

regions of polycarbonate and polyethylene was used as ρ. In addition, it was assumed in calculations that

$$R_{cl} = R_{WS}, \tag{92}$$

$$D = d_f. \tag{93}$$

The absolute magnitudes and the patterns of temperature variation of the parameters r_{cl} and a are in good agreement. Some scatter in the a values relative to r_{cl} is due to the inaccuracy in the determination of d_f using Eqn (23), caused by the power dependence of a on D, which markedly affects the accuracy of comparison.

Thus, it can be inferred that experimental results also indicate the obligatory existence of regions of local order in the structure of an amorphous polymer in terms of the DLA model. The structure of amorphous polymers can also be studied using the method of autocorrelation functions [176]

$$C(r) = \langle p(r') - p(r' + r)\rangle, \tag{94}$$

where $p(r')$ and $p(r' + r)$ are probabilities that particles composing a cluster are located at points r' and $r' + r$ (the probability is equal to unity when the point does contain a particle and to zero when no particle is present). The autocorrelation function for distances r greater than several lattice spacings can be represented by the scaling relation [186]

$$C(r) \propto r^{-\alpha}, \tag{95}$$

where

$$\alpha = d - D. \tag{96}$$

In the case of a linear autocorrelation function, having determined α, one can estimate the fractal dimension D of the object.

The autocorrelation function for the structure of an amorphous polymer (in particular, polycarbonate) is shown schematically in Fig. 37; the density variation is presented as a function of distance, the reference point ($r = 0$) being placed at the centre of a local order region (see Fig. 35). Over an interval from 0 to r_{cl} the ρ value remains constant and equal to the density of the region of local order, which has been assumed, as a first approximation, to be equal to the ρ_{cr} value for crystalline polycarbonate.[187] In the range from r_{cl} to R_{cl}, the density is supposed to decrease linearly to reach ρ_{min}, which is estimated as follows. Litt *et al.*[187] have reported the averaged density of amorphous polycarbonate ρ_a,

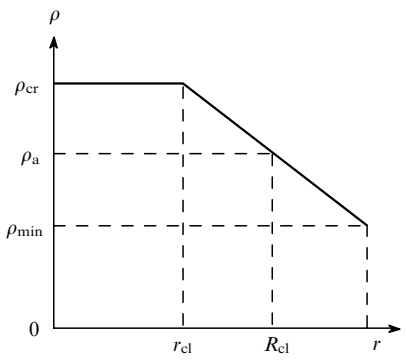


Figure 37. Autocorrelation function $\rho(r)$ for polycarbonate. The explanations are in the text.

which corresponds to the centre of the sloping section in Fig. 37. From simple geometric considerations, we obtain

$$\rho_{min} = \rho_a - (\rho_{cr} - \rho_a). \tag{97}$$

Now one can estimate the α value from the relation

$$(\rho_{cr} - \rho_{min})^{-\alpha} \simeq \left(\frac{R_{cl}}{2} - r_{cl}\right)^{-\alpha}, \tag{98}$$

and then calculate the d_f value for the polymer structure using Eqn (96) because modelling of this structure by a WS cluster assumes that equality (93) is valid.[178]

The temperature dependences of the fractal dimension of the polycarbonate structure obtained experimentally and calculated in terms of the WS model taking account of relations (95) and (98) are presented in Fig. 38. It can be seen that the results correspond rather well to each other. However, the agreement can be improved by using so-called 'true' yield point. Kozlov *et al.*[166] determined d_f for polycarbonate at 293 K using five different procedures; the average value was found to be $d_f \simeq 2.51$. This result is in good agreement with the value $d_f \simeq 2.56$ determined for 293 K in terms of the WS model.

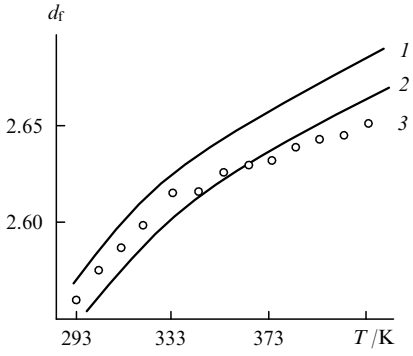


Figure 38. Fractal dimensions d_f of the structures of polycarbonate (*1*, *2*) and WS cluster (*3*) *vs.* temperature.
Determined with allowance for real (*1*) and 'true' (*2*) yield point.

Recalling that the quasi-equilibrium state of a polymer structure is characterised, in the general case, by $d_f = 2.5$, the same fractal dimension is typical of a WS cluster in a three-dimensional space when $N \to \infty$.[186] Therefore, below we consider the correspondence between the conditions of formation of a quasi-equilibrium state in the cluster model of an amorphous polymer structure and in the WS model. The modification of the WS model discussed above (growth on a large number of 'seeds') [177] uses the term 'diffusion distance' ξ, which depends on the local environment of each 'seed'. The growth of a WS cluster

continues until the condition $\xi \simeq R_{cl}$ is attained. The ξ and R_{cl} values are related to the concentration of free particles (c_{fr}) in the following way:[178]

$$\xi \simeq c_{fr}^{-1} R_{cl}^{D-d+2}. \quad (99)$$

Taking into account the condition for termination of the cluster growth, it can be written that

$$c_{fr} \simeq R_{cl}^{D-d}. \quad (100)$$

This relation allows one to determine the concentration of free particles at the moment when the WS cluster stops growing having reached the size R_{cl} (subsequently, this concentration is designated by c_{WS}) or when the quasi-equilibrium state in terms of the WS model has been attained because in this case, too, the diffusion growth is restricted by interaction of the neighbouring WS clusters.

The concentration of particles in the cluster can be determined in terms of the cluster model.[173] Using relations (45) and (53), d_f can be related to the fraction of clusters φ_{cl}. Assuming that $d_f = 2.5$, one can estimate the φ_{cl} value for the quasi-equilibrium state of polymers.[15]

The R_{cl} value in the model[178] is limited by the number of 'seeds', which is, in turn, equal to the number of WS clusters, n_{WS}. According to the cluster model, the number of statistical segments incorporated in the regions of local order per unit volume of the polymer is assumed to be equal to the density of cluster network V_{cl}. The functionality F of such a region is the number of chains protruding from it. Since this region (cluster) is an analogue of a crystallite with extended chains, the number of segments in one cluster is equal to $F/2$. The number of regions of local order N_{cl}, equal to n_{WS}, in unit volume of the polymer can be found from the equation[113]

$$N_{cl} = \frac{2V_{cl}}{F}. \quad (101)$$

In addition to the cluster network of entanglements, polymers are known to contain a network of traditional 'loops'; unlike the cluster network, the latter is retained above T_g.[146] The numbers of entanglements in this network, determined above T_g, have been reported (see, for example, Refs 62, 76, 188). The density of the network of these 'loops' (V_{en}) can be found from the equation

$$V_{en} = \frac{\rho N_A}{M_{en}}, \quad (102)$$

where M_{en} is the molecular mass of the chain between entanglements.

Figure 39 illustrates the relationship between the N_{cl} and V_{en} values for eight polymers. It can be seen that these parameters correspond to each other both in magnitude and in the pattern of variation. The rather large scatter is due to the discrepancies between the M_{en} values taken from different sources for the same polymer [for instance, for polyethylene, $M_{en} = 737$ g mol^{-1} (see Ref. 62) or 1900 g mol^{-1} (see Ref. 188)]. Nevertheless, under the assumption that $N_{cl} \simeq V_{en}$, the V_{en} value can be identified as the density of 'seeds' and the R_{cl} value can be found using Eqn (30).

The use of dimensional R_{cl} values in relation (100) results in the c_{WS} value being dependent on the dimension of R_{cl}. Therefore, the lower limit (b) at which the fractal properties are manifested ($b \simeq 0.5$ nm[173]) was chosen as the scale, and the dimensionless parameter R_{cl}/b was used in Eqn (100). When a different b value is employed, c_{WS} somewhat changes but the trend of its variation is retained.

It has been shown[189] that the minimum value $d_{f\,min} = 2.5$ is typical only of polymers with $C_\infty = 3$. The $d_{f\,min}$ value can be determined by modification of the equation[190]

$$\frac{d_{f\,min}}{3(3 - d_{f\,min})} + \frac{4}{3} = C_\infty. \quad (103)$$

For polymers with $C_\infty > 3$, the calculation gives incorrect φ_{cl} values (greater than unity). Therefore, the $d_{f\,min}$ values found for polymers using Eqn (103) are greater than 2.5. Thus, the chain rigidity has a substantial influence on the formation of the polymer structure.

Only segments incorporated in the loosely packed matrix have the opportunity to join the regions of local ordering. Thus, in terms of the WS model, it is these segments that should be considered as free particles. Therefore,

$$c_{sf} = 1 - \varphi_{cl} = \varphi_{lp},$$

where φ_{lp} is the volume fraction of the loosely packed matrix.

Figure 40 illustrates the good correspondence between the c_{WS} and c_{sf} values for twelve polymers, which attests that the interpretations of the quasi-equilibrium state of the polymer structure in the cluster model[173] and in the WS model[178] are equivalent. The c_{WS} values are somewhat greater than c_{sf} because the scale b was chosen arbitrarily.

Thus, the concepts of quasi-equilibrium state involved in the DLA and cluster models of the structure of amorphous polymers are similar in physical essence, the quantitative estimations in terms of these two models providing consistent results. The

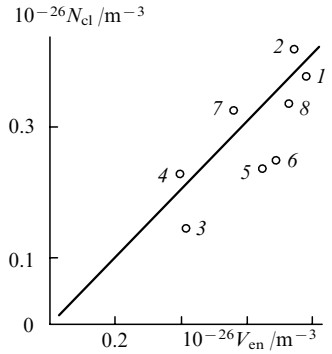


Figure 39. Relationship between the densities of clusters N_{cl} and the network of macromolecular 'loops' V_{en} for various polymers;
(*1*) poly(ethylene terephthalate), (*2*) polyamide-6, (*3*) polyethylene, (*4*) polypropylene, (*5*) polystyrene, (*6*) poly(methyl methacrylate), (*7*) poly(vinyl chloride), (*8*) polycarbonate.

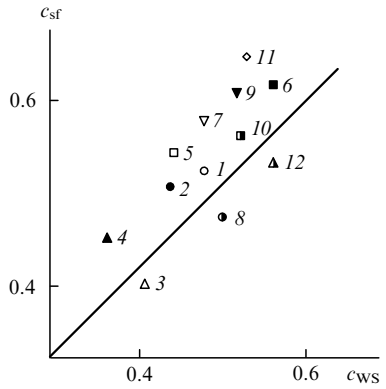


Figure 40. Relationship between the concentrations of free particles c_{WS} and statistical segments in the loosely packed matrix c_{sf} for the quasi-equilibrium state;
(*1*) polyethylene, (*2*) poly(methyl methacrylate), (*3*) polystyrene, (*4*) polytetrafluoroethylene, (*5*) polypropylene, (*6*) polycarbonate, (*7*) poly(ethylene terephthalate), (*8*) poly(vinyl acetate), (*9*) poly(ethylene oxide), (*10*) polycaprolactam, (*11*) polyestersulfone, (*12*) poly(vinyl chloride).

macromolecular 'loops', which restrict the mobility of polymer chains act as the 'seeds' in the WS model.[178]

3. Order and fractality in polymers

The temperature dependences of V_{cl} for different polymers are similar. Raising the temperature results in a decrease in V_{cl}, the rate of thermofluctuational decomposition of clusters sharply increasing as T approaches T_g (or T_m). This general regularity is illustrated by the plots for V_{cl} *vs.* testing temperature for polycarbonate, poly(methyl methacrylate) and high-density polyethylene (Fig. 41). Note that similar temperature dependences are obeyed by the mechanical properties of polymers (elastic modulus, yield point, *etc.*).[191] This similarity implies the possibility of superposition of the $V_{cl}(T)$ curves for different polymers, which is due to the common pattern of variation of the degree of local ordering *vs.* temperature. Below we construct this superposition and consider some its consequences in terms of the cluster model resorting to percolation theory and fractal analysis.[60]

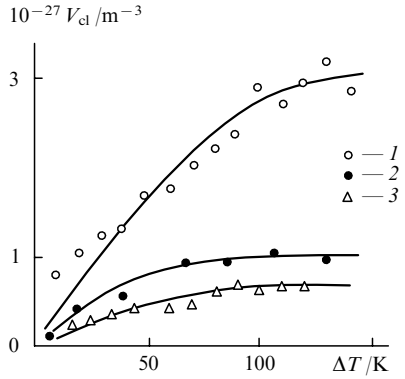


Figure 41. Density of the cluster network of entanglements V_{cl} *vs.* reduced testing temperature $\Delta T = T_g - T$ for polycarbonate (*1*), poly(methyl methacrylate) (*2*) and $\Delta T = T_m - T$ for high-density polyethylene (*3*).[60]

The dependences of V_{cl} on the reduced temperature $\Delta T = T_g - T$ for some polymers follow similar patterns (see Ref. 41); therefore, a scaling relation of the following type can be applied:

$$V_{cl} \propto \Delta T^x, \tag{104}$$

where x is a generalised index.

However, the degree of local ordering is reflected more precisely by the relative portion of clusters φ_{cl}, determined from Eqn (53). An obvious advantage of Eqn (53) is the fact that it includes the main molecular characteristics of polymers. Figure 42 shows the $\ln\varphi_{cl}(\ln\Delta T)$ plots for the three polymers mentioned above and for the epoxy polymer EP-1, which are approximated by a common straight line. It can be easily seen that

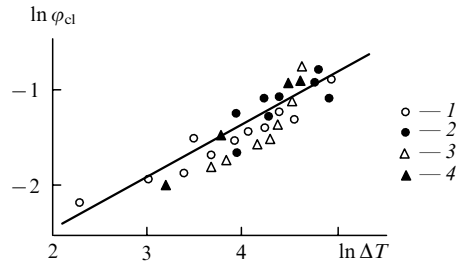


Figure 42. Relative portion of the clusters φ_{cl} *vs.* reduced testing temperature ΔT for polycarbonate (*1*), poly(methyl methacrylate) (*2*), high-density polyethylene (*3*) and EP-1 (*4*).[60]

these data comply well with the known relation of percolation models in the case of critical transition [162]

$$P_\infty \propto (T_g - T)^\beta. \tag{105}$$

In this interpretation, the φ_{cl} value corresponds to the 'power' of an infinite cluster, *i.e.* the probability P_∞ that a unit belongs to the infinite cluster. Thus, at T_g (or T_m), the cluster network of entanglements appears (or vanishes); simultaneously, the structure of a vitreous polymer sample as a system is formed (or destroyed). Several other important points related to the possibility of describing a polymer structure in terms of Eqn (105) deserve attention. In the cluster model, the statistical segment l_{st} is taken as the 'section of rigidity' of a chain. The l_{st} value is several times smaller than the Kuhn segment length A, which characterises the rigidity of a freely jointed chain.[91] When the A value is chosen as the 'section of rigidity', the φ_{cl} values prove to be greater than unity in most cases, which is devoid of physical meaning. The relationship between A and l_{st} can be written in the following form:

$$l_{st} = A\cos\frac{\theta_v}{2}, \tag{106}$$

where θ_v is the bond angle.

Thus, the shorter length of the chain section of rigidity l_{st} in the vitreous state is due to the conformational rearrangements peculiar to this state.

In the case of amorphous-crystalline high-density polyethylene, the reduced φ'_{cl} value was used; this parameter characterises φ_{cl} with respect to the whole polymer bulk rather than to the amorphous phase alone

$$\varphi'_{cl} = \frac{\varphi_{cl}}{1-k}, \tag{107}$$

where k is the degree of crystallinity.

The relation modified for the case of amorphous-crystalline polymers is represented by Eqn (53). Using Eqns (53) and (23), one can elucidate the relationship between d_f and φ_{cl}

$$d_f = d - 5.98\times10^{-10}\left(\frac{\varphi_{cl}}{C_\infty S}\right)^{1/2}, \tag{108}$$

where S is expressed in Å^2.

As has been shown above, Eqn (45) provides the minimum values for the fractal dimension of structure (d_f^t) possible for a given polymer, which are in good agreement with the d_f^0 values (see Table 1). Hence, by substituting d_f^t or d_f^0 into Eqn (108), one can estimate the limiting degree of local ordering (φ_{cl}^0) possible for a given polymer as a function of the most important molecular characteristics of the polymer, C_∞ and S. When the temperature decreases below T_0 (at which the φ_{cl}^0 value is attained), the degree of local ordering does not change; therefore, T_0 can be regarded as an analogue of the temperature T_∞ at which the polymer reaches a constant free volume.[106, 173, 191, 192] Meanwhile, T_0 can be found from Eqn (104) provided that $\varphi_{cl} = \varphi_{cl}^0$. The T_0 and T_∞ values thus obtained, together with the temperatures of transition to a state with a constant value of density fluctuations T^*,[106, 193] for eight polymers are listed in Table 3. It can be seen that T_0 and T_∞ are in good agreement for all polymers except polycarbonate, for which the calculation gave $\Delta T = 670$ K, which has no physical meaning. For real polymers, the tendency towards a thermodynamically more equilibrium state should be counterbalanced at a certain point by the force of chain 'tightening.' Therefore, the value $d_f = 2.5$ should be used instead of d_f^t. In addition, the value $\varphi_{lp} = 1$ (*i.e.* $\varphi_{cl} = 0$) is attained at $d_f = 2.92$ rather than at $d_f = 3$, as could be suggested in view of Eqn (108). With allowance for these corrections, calculation in terms of Eqn (105) affords $T_0 \simeq 318$ K for polycarbonate, which is consistent with the value $T_\infty = 323$ K (see Table 3). The correspondence between T_0 and T^* is poorer than that between T_0 and T_∞ but the patterns of their variation for polymers fully coincide.

Table 3. Temperatures of the transitions to the 'frozen' free volume T_∞, quasi-equilibrium state T_0 and a constant density fluctuation T^*.

Polymer	T_∞/ K	T_0/ K	T^*/ K
Poly(ethylene terephthalate)	280	300	220–250
Polyamide-6	277	304	200
Polyethylene	227	243	140–150
Polypropylene	227	199	210
Polystyrene	324	320	270
Poly(methyl methacrylate)	290	269	250–280
Poly(vinyl chloride)	270	333	220
Polycarbonate	323	318	200–220

The following empirical relation between the change in the specific Gibbs function of the formation of the supermolecular structure ΔG during the self-assembly of the cluster structure and φ_{cl} has been derived [194]

$$\Delta G \propto \varphi_{cl}\,. \tag{109}$$

Substitution of this relation into Eqn (108) gave the expression

$$\Delta G \propto C_\infty S(3 - d_f)^2. \tag{110}$$

The ΔG value for the supercooled liquid–solid nonequilibrium phase transition has been reported.[195] It follows from relation (110) that $\Delta G = 0$ when $d_f = 3$, *i.e.* when the fractal properties are lost. In other words, the fact that fractal structures are formed only in nonequilibrium processes has been confirmed once again.[12]

4. The possibility of numerical modelling of polymer properties

Little is known about a polymer synthesised from monomers or prepared by curing an oligomer; as a rule, the known data include the trademarks of monomers, oligomers, and curing agents and their ratios. Evidently, in this situation, for example, in the case of network polymers, the main initial parameter — cross-linking density ν_s — can be either calculated [154] or determined experimentally.[192] In the latter case, the molecular mass of the chain section between the cross-linking points M_s is calculated using the equation

$$\frac{1}{M_s} = \frac{F_i m}{2W}, \tag{111}$$

where F_i is the functionality of the curing agent, m is the number of moles of the curing agent in the sample, and W is the sample weight.

Comparison of the $T_g(\nu_s)$ plots for different epoxy polymers for which the ν_s values were determined by both methods mentioned above shows that the experimental values are somewhat lower than the calculated ones. This discrepancy can be eliminated by introducing the correction factor C. The discrepancy is due to two reasons; one reason is the use of different batches of epoxy resins and curing agents and the other reason is that the calculation implies completeness of the curing reaction, *i.e.* that the curing agent has been entirely consumed, which does not occur in reality.

Apart from ν_s, it is necessary to estimate the cross-section area of the macromolecule S and the length of a real bond in the backbone l_0. The S value is either taken from reference data (if they do exist) or estimated by comparison with the S value of a linear polymer with a similar chemical structure. For example, the chemical structures of the epoxy resins and polycarbonate are similar because they both are based on bisphenol A. Therefore, the value $S = 0.31$ nm^2, determined for polycarbonates, was used for these epoxy polymers.[76] Experimental estimates have shown [71] that this approximation is correct to within $\sim 5\%$. As regards the l_0 value, it characterises a class of polymers rather than a particular polymer, which makes its determination easier. Since epoxy resins are heterochain polymers, $l_0 = 0.125$ nm.[76]

Using the above parameters, one can estimate the length of the section of a macromolecule between chemical cross-linking points and the distance between chemical cross-linking points.[14] The subsequent stage is to solve a set of three equations with three variables, namely, the characteristic ratio C_∞ and the fractal dimensions of the macromolecule section between chemical cross-linking points D and of the cluster structure d_f. By solving this set of equations, one can find these structural characteristics of the epoxy polymers. After that, the Poisson coefficient should be found from Eqn (23) and the cluster network density V_{cl} should be determined from the relation

$$\mu = 0.5 - 2.98 \times 10^{-10}(V_{cl}\, l_0)^{1/2}. \tag{112}$$

Finally, the relative portion of clusters is calculated as

$$\varphi_{cl} = \frac{V_{cl}}{V} \tag{113}$$

where V is the polymer volume.

For the loosely packed matrix,[60]

$$\varphi_{lp} = 1 - \varphi_{cl}\,. \tag{114}$$

Thus, we have obtained a complete set of characteristics of the molecular, topological, and supermolecular levels of the structure of cross-linked polymers, which permits one to model and predict their properties. The properties chosen include three characteristics for applications (elastic modulus E, yield point σ_p and glass transition temperature T_g), which are needed to develop new materials, and three characteristics which are regarded conventionally as theoretical (Grüneisen parameter γ, thermal expansion coefficient a_t and yield strain ε).

It should be taken into account that one order parameter (for example, φ_{cl}) is inadequate to describe the structure and properties of an amorphous polymer. It has been shown in relation to linear polymers [196] that the need for a second order parameter is due to the thermodynamic nonequilibrium of the loosely packed matrix. In other words, $f_{fv} \neq f'_{fv}$. Therefore, a second order parameter was introduced for linear polymers, namely, $(f'_{fv} - f_{fv})/f_{fv}$. In the case of cross-linked polymers, the constant contribution to f_{fv} caused by the presence of chemical cross-linking points should be additionally taken into account as f^*_{fv} ($f^*_{fv} = 0.024$, see Refs 70, 185). The use of percolation models [197] results in the relation

$$G \propto \left(\varphi_{cl} - \frac{f'_{fv} - f^*_{fv} - f_{fv}}{f_{fv}}\right)^A, \tag{115}$$

where G is the shear modulus, $A \simeq 1.5$.

Having determined f'_{fv} from relation (70) and f_{fv} from relation (55), one can find the shear modulus and then, using Eqn (44), the elastic modulus.

The relation for determining the yield point derived using relations (23) and (44) has the form

$$\sigma_p = \frac{E(3 - d_f)}{3d_f}\,. \tag{116}$$

The σ_p value can also be estimated using the equation [198, 199]

$$\sigma_p = \frac{3^{1/2} G \boldsymbol{b} (l_{st} V_{cl})^{1/2}}{2\pi}, \tag{117}$$

where $\boldsymbol{b}$ is the Burgers vector, determined from the empirical relation [129]

$$\boldsymbol{b} = \left(\frac{52.2}{C_\infty}\right)^{1/2}. \tag{118}$$

The glass transition temperature T_g can be found either using an empirical equation [71] or in terms of the fractal approach to glass transition. This is done either using a general model or a

model which takes into account the stabilising influence of chemical cross-links *via* the factor $v_s^{1/2}$ (see Ref. 200).

The Grüneisen parameter γ can be determined by one of the following methods: calculation in terms of relation (69) using the parameter D_f (equal to D_{ffv}), determined previously from Eqn (39); calculation in terms of Eqn (68); or calculation using the relation

$$\gamma = \frac{9\pi^2}{4(S^{1/2} + l_0)(l_{st} V_{cl})^{1/2}} - 0.25. \quad (119)$$

The thermal expansion coefficient a_t can be found from the equation

$$\gamma = \frac{3 + a_t T(3 + a_t T)}{6a_t}. \quad (120)$$

The yield strain ε is found from relation (67) provided that $\varepsilon = \varepsilon_c$.

Thus, the approach making use of the cluster model of the structure of amorphous polymers and fractal analysis provides the possibility of numerical modelling of the structures and properties of network polymers. An obvious advantage of this procedure is the fact that only v_s and S are actually used as calculation parameters. It should be noted that the simplicity of choosing the input data is combined with the strict physical interpretation of these data and, hence, no empirical adjusting coefficients are required.

IV. Experimental determination of the fractal dimension

1. A brief survey of the methods

Various methods are used to determine the fractal dimension,[61,201] which can be conventionally divided into two groups: fractographical and physical methods, based on the relationship between the fractal dimension and physical properties. The former group includes the methods of horizontal sections (cut islets),[202–207] vertical sections,[13,208–211] profile Fourier analysis,[203,212] decentration, expansion, and cell counting,[61,213] similarity transformation,[214,215] *etc*. The fractographic methods used to gain fractal information on the irregularity of fractured surfaces make it possible to investigate profiles as horizontal or vertical sections of the surface. This requires additional hypotheses to attain reliability of the relationships between the surface fractal properties and size.[208,216,217]

The main goal of fractographic measurements is to determine the fractal dimension of, for example, chipped (fractured) surface and the limits in which the surface exhibits fractal properties. The main problem is the legitimacy of measuring the fractal dimension of self-affine fractured surfaces. The horizontal profile of a fractured surface can be statistically self-similar but the vertical profile is usually self-affine.[218,219] Thus, the horizontal and vertical surface sections have absolutely different scaling characteristics, which need to be estimated using different procedures of measurements.

In the case of statistically self-similar horizontal contours, any sensible procedure for determination of the fractal dimension should give the same value.[87] The question is how this fractal dimension is correlated with the fractal properties of the self-affine fractured surface. Self-affine vertical profiles can be characterised by many fractal dimensions, for example, local and global fractal dimensions. The latter are always equal to the topological dimension of the profile, while the local dimensions of the profile irregularities can be represented as exponential functions.[220]

The second group of methods comprises various physical methods used most often for fractal analysis of surfaces (mainly, fractured surfaces). They include porometry,[211,222] scattering procedures (*e.g*., small-angle neutron scattering),[13] optical diffraction methods,[13,61,182,223] secondary electron emission measurement,[13] adsorption–desorption measurements (adsorption probe method),[13,224–227] methods of thermodynamics,[228] the deposit experiment method,[229] electro- and thermochemical methods,[229,230] NMR measurements of the pore distribution,[231] procedures based on the results of mechanical measurements,[61,232] *etc*.§

2. Small-angle X-ray diffraction

As an example, we shall consider the practical application of one method, small-angle X-ray scattering (SAXS), which is widely used to study the fractal structure of solids.[227,233–245] Polymers are mainly studied by this method during cross-linking in solutions.[233–235] The theoretical grounds of the method have been developed fairly well by now.[238,241,242] The fractal structures of block polystyrene, poly(methyl methacrylate), and polycarbonate have been studied by the SAXS method.[153] These particular polymers were chosen because they are often used as model systems and, therefore, they are well characterised and because the structures of macromolecules[76] and, as a consequence, the properties of these polymers are different.[244]

The use of the SAXS method is based on the characteristic power dependence of the scattering intensity I on the scattering vector

$$I(\boldsymbol{k}) \propto \boldsymbol{k}^{-x}, \quad (121)$$

where x is a Porod index, the interpretation of which depends on the nature of the scattering source

$$\boldsymbol{k} = 4\pi\lambda^{-1} \sin\frac{\theta}{2}, \quad (122)$$

where λ is the X-ray radiation wavelength and θ is the scattering angle.[224]

In the case of bulk fractals (*i.e*. structures like polymers), this index coincides with the fractal dimension of the structure d_f.[224,242]

For a fractal phase interface with the dimension D_i, the following relation holds:[238]

$$I(\boldsymbol{k}) \propto \boldsymbol{k}^{D_i - 6}, \qquad 2 < D_i < 6. \quad (123)$$

Figure 43 shows the $\ln I(\ln k)$ plots, while Fig. 44 presents the dependences of $\ln I$ on k^2 for the polymers mentioned above.[245] Two linear sections present for each polymer of Fig. 43 point to the existence of two regions with different fractal dimensions. These plots differ from the analogous plots for silicates, for which the slope of the $\ln I(\ln k)$ plots increases discretely with an increase in k (which implies the loss of fractal properties), but are similar to the dependences obtained for amorphous chalcogenide films.[242] To identify the structural regions responsible for the observed change in the slope, the cluster model for the structure of

§ Experimental methods for determining the fractal dimension are considered in detail, for example, in a monograph.[237]

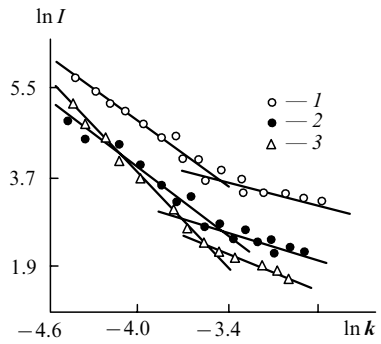


Figure 43. SAXS intensity *vs*. scattering vector $\boldsymbol{k}$ for poly(methyl methacrylate) (*1*), polystyrene (*2*), polycarbonate (*3*).[39]

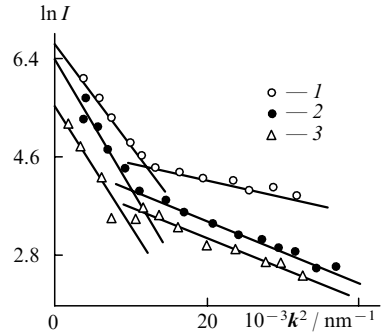


Figure 44. SAXS intensity *vs.* $\boldsymbol{k}^2$ for poly(methyl methacrylate) (*1*), polystyrene (*2*), polycarbonate (*3*).[39]

amorphous polymers was used. The region of local order and the sections of macromolecules protruding from it should be considered as the fractal cluster.[125] The size of this cluster is twice the distance between the regions of local order, and its fractal dimension characterises the structure of the whole polymer, which is a set of generalised fractal clusters. Another structural region is represented by the loosely packed matrix located between the local order regions; all the fluctuation free volume is accumulated in this region. The R_{cl} values for the polymers considered are listed in Table 4. Using the plots presented in Fig. 44 one can calculate the Guinier radii.[245] Attention is drawn by the facts that R_G and R_{cl} are close in magnitude and that R_G increases twofold on passing from one linear section to the other (Fig. 43), which corresponds to the transition from R_{cl} to $2R_{cl}$. This suggests that the R_G and R_{cl} values reflect the same structural parameter. The condition for the fractality of particles which scatter X-rays in the range of small angles is known[224] to be represented by the inequality $R_G\boldsymbol{k} \geqslant 1$.

Table 4. Structural and fractal characteristics of amorphous polymers.

Polymer	R_{cl}/ nm	R_G/ nm		d_{fp}	D_{fp}	d_f	D_f
		$\boldsymbol{k} < 0.028^{-1}$	$\boldsymbol{k} > 0.028^{-1}$				
Polystyrene	4.1	10.0	5.0	2.80	5.12	2.75	5.0
Poly(methyl methacrylate)	3.7	10.0	5.0	2.80	5.20	2.70	4.33
Polycarbonate	3.0	8.0	4.0	2.40	4.40	2.62	3.63

The presence of two R_G values implies the existence of a boundary between fractal structural regions, which can be found from the condition $R_G\boldsymbol{k} \geqslant 1$. For a fractal cluster with the size $2R_{cl} \simeq 7.0$ nm, this corresponds to $\boldsymbol{k} \simeq 0.00143$ nm^{-1} or $\ln \boldsymbol{k} \simeq 4.25$, which is the upper limit of fractality of the polymer structure. When $R_G \simeq R_{cl} \simeq 3.5$ nm, we have $\ln \boldsymbol{k} \simeq -3.56$, which is consistent with the $\ln \boldsymbol{k}$ value at which the slope of the plots in Fig. 43 changes.

Thus, the section of the dependence of $\ln I$ on $\ln \boldsymbol{k}$ for $\ln \boldsymbol{k}$ ranging from 4.25 to -3.56 can be associated with the cluster structure of an amorphous polymer and the section for $\ln \boldsymbol{k} > -3.56$ is matched by the loosely packed matrix.

The existence of these boundaries is due to a known feature of real fractals — the fractal behaviour is realised only within a definite scale range. Several ranges have been determined for amorphous solids;[242] we shall distinguish two of them which correspond to the $\boldsymbol{k}$ values used. If the size of a cluster of pores ¶ is designated by η_p and the size of a pore is designated by a_p, the dimension of structural elements will be estimated in the following ranges of $\boldsymbol{k}$. When $\boldsymbol{k} < \eta_p^{-1}$, the dimension of the structure itself is determined, while for $\eta_p^{-1} < \boldsymbol{k} < a_p$, the dimension of the cluster of pores is found. It has been shown[189] that the fluctuation free volume in a polymer is a fractal object, its dimension being equal to the dimension of the regions of localisation of excess energy D_f.[246] In other words, D_f characterises the degree of energy excitation of the loosely packed matrix. The dimensions d_f and D_f can be found from relations (23) and (39), respectively.

The d_{fp} values estimated from Eqn (123) with allowance for the slope of the plots shown in Fig. 43 ($\ln \boldsymbol{k}$ is -4.25 to -3.56) are summarised in Table 4. The d_f values found using Eqn (23) are given for comparison. The fact that the values thus obtained are close confirms the validity of this interpretation.

The slope of the plot sections for $\ln \boldsymbol{k} > -3.56$ is close to unity; it cannot be interpreted as the fractal dimension of a structural element if for no other reason than its magnitude. Therefore, Eqn (123) was used to determine the fractal dimension. Comparison of the D_{fp} and D_f values obtained in this way [see Eqn (39)] showed that they are in good agreement (see Table 4). Note that a slope of the order of unity (-0.75 to -0.80) has also been obtained for a similar $\boldsymbol{k}$ range for amorphous chalcogenide films; however, this result was not interpreted.[242]

The condition $R_G\boldsymbol{k} \geqslant 1$ is usually obeyed for larger angles in the small-angle region. However, in the case of relatively large structural elements, the region of fractality and the Guinier region can overlap. Apparently, this overlap also takes place for the polymers under consideration. The range of linearity of the plots shown in Figs 43 and 44 is $(1-3) \times 10^3$ nm^{-1} and $R_G \simeq 10$ nm, *i.e.* the product $R_G\boldsymbol{k}$ falls in the range from 1 to 3. The overlap of the fractality and Guinier regions may imply a relationship between the fractal dimension d_f and the Guinier radius R_G. This can be demonstrated analytically in the following way. According to the small-angle Guinier approximation, the following relation holds:[245]

$$I = I_0 \ln\left(-\frac{R_G^2 \boldsymbol{k}^2}{3}\right), \tag{124}$$

while in the range of the Porod large angles, the relation[153]

$$I = C\boldsymbol{k}^{-d_f}, \tag{125}$$

is valid, where I_0 and C are constants. For equal I, there exists a formal relationship between d_f and R_G[153]

$$d_f = \frac{(R_G^2/3)\boldsymbol{k} - \ln(I_0/C)}{\ln \boldsymbol{k}}. \tag{126}$$

It is noteworthy that this relationship is not obligatory in terms of the cluster model. An increase in R_G means an increase in the distance between the clusters, a decrease in V_{cl}, an increase in μ, and the corresponding increase in d_f, which is reflected by relation (126).

We would like to note yet another important aspect of determination of d_f by the SAXS method. Based on the data of previous publications,[238,246] Novikov *et al.*[167,182] estimated the d_f values for amorphous vitreous polymers to be 2.0–2.2. In another study,[247] polystyrene has been tested at 16 K; as shown above, transfer of this result to the temperature range of about 293 K is improper. Studies of the silicate colloid aggregates[224,241,248] showed that their porosity influences appreciably the d_f value. Thus pressing (*i.e.* an increase in the density) of samples results in markedly higher d_f ranging from 2.55 to 2.65.[241] Feder[13] obtained $d_f = 2.56$ for protein aggregates. These results are in good agreement with the data obtained in terms of Eqn (23) and with the above SAXS data. Therefore, any estimates assuming *a priori*, without sufficient grounds, $d_f \simeq 2$ for amorphous vitreous polymers can induce substantial errors, for example, in the calculation of d_s.[167,182]

¶ In amorphous polymers, the term 'pores' is used in relation to microcavities of free volume and the term 'cluster of pores' refers to the loosely packed matrix in which they are concentrated.

Thus, the SAXS methods make it possible to confirm the fractality of different structural components of amorphous vitreous polymers and to measure their fractal dimensions. The upper limit of the fractal behaviour of polymers, equal to $\sim 2R_{cl}$, is also in good agreement with the estimate of this value reported by Novikov *et al.*[167]

V. Conclusion

A feature distinguishing the fractal approach from the physical models of polymer synthesis developed previously is that it takes into account the structure of the macromolecular coil, which determines the polymer structure, and characterises simultaneously the fractal dimension of the coil and the particular mechanism of the coil formation. The results obtained along this line indicate that the growth of macromolecules during the polymer structure formation stops when the macromolecular coil has reached the density of the reaction medium rather than due to exhaustion of the chemical reactants, *i.e.* the reaction is terminated by purely physical factors. This conclusion is impossible in terms of the Euclidean geometry.

Based on fundamental physical principles, the multilevel polymer structure has been described and the equations relating the molecular characteristics, topology, and parameters of the supermolecular structure of polymers are analysed. The application of principles of nonequilibrium thermodynamics and treatment of vitreous polymers as structurally inhomogeneous solids provided understanding of the fact that the mechanical energy applied during deformation is 'pumped' into the loosely packed regions of the polymer and dissipated in the closely packed regions (clusters). The dissipation of mechanical energy induces shear stress in the clusters; the clusters lose their stability, which causes the polymer to yield.

Analysis of the concept of the fluctuation free volume in a vitreous polymer has shown that it possesses fractal properties; hence, the microcavities composing this volume can be modelled by a D_{ffv}-dimensional sphere. The microcavity size is restricted by the volume in which the energy of thermal fluctuations needed for their formation is accumulated. It is shown that 'stretching' of macromolecules hampers an increase in the degree of ordering. When the thermodynamic forces inducing these effects are counterbalanced, the polymer reaches a certain quasi-equilibrium state, which is explained by a density fluctuation above a particular temperature below the glass transition temperature. The introduction of the concept of the quasi-equilibrium state of polymers provides a better understanding of several experimental findings.

The results of modelling the polymer structure using percolation and aggregation theory showed that the structure formed at the glass transition temperature is a percolation cluster. Glass transition is assumed to be a phase transition. The fractal dimension of these structures is determined by the disorder generated by deterministic chaos. Simultaneously, it was shown that the polymer structure can be modelled by a modified model of the diffusion-limited irreversible aggregation. The superposition of the cluster volume – temperature curves for amorphous and amorphous-crystalline polymers and the relationship between fractality and local order in the structure of vitreous polymers were described within the framework of the cluster model resorting to the percolation theory. The importance of calculation of the properties of polymers is demonstrated by presenting a procedure based on the cluster model of the amorphous state structure and fractal analysis. This procedure allows one to perform numerical modelling of properties of, for example, cross-linked polymers. An obvious advantage of this method is the simplicity of choosing the input data in combination with strict physical interpretation and the absence of adjusting coefficients.

This brief survey of the methods of determination of the fractal dimension and the practical application of the SAXS procedure for determining the fractal dimension demonstrates the prospects for using the fractal approach for the investigation of the structure and properties of polymers.

References

1. B B Mandelbrot *The Fractal Geometry of Nature* (San Fransisco: Freeman, 1982)
2. D Stauffer, H E Stanle *From Newton to Mandelbrot* (New York: Academic Press, 1996)
3. P R Massopust *Fractal Function, Surface and Wavelets* (New York: Academic Press, 1996)
4. G M Bartenev, S Ya Frenkel' *Fizika Polimerov* (The Physics of Polymers) (Leningrad: Khimiya, 1990)
5. S F Edwards, T Villgis *Polymer* **28** 375 (1987)
6. E Hornbogen *Int. Mater. Rev.* **34** 277 (1989)
7. V S Ivanova, A S Balankin, I Zh Bunin, A A Oksogoev *Sinergetika i Fraktaly v Materialovedenii* (Synergetics and Fractals in Materials Technology) (Moscow: Nauka, 1994)
8. M H Bessendorf *Int. J. Eng. Sci.* **25** 667 (1987)
9. V V Korshak, S V Vinogradova *Neravnovesnaya Polikondensatsiya* (Nonequilibrium Polycondensation) (Moscow: Nauka, 1972)
10. V G Baranov, S Ya Frenkel', Yu V Brestkin *Dokl. Akad. Nauk SSSR* **290** 369 (1986) [a]
11. R Rammal, D Toulouse *J. Phys. Lett.* **44** L13 (1983)
12. B M Smirnov *Fizika Fraktal'nykh Klasterov* (The Physics of Fractal Clusters) (Moscow: Nauka, 1991)
13. J Feder *Fractals* (New York: Plenum, 1988)
14. V U Novikov, G V Kozlov *Usp. Khim.* **69** 378 (2000) [*Russ. Chem. Rev.* **69** (2000)]
15. T A Witten Jr, L M Sander *Phys. Rev. Lett.* **47** 1400 (1981)
16. P Meakin *Phys. Rev. Lett.* **51** 1119 (1983)
17. M Kolb, R Botet, R Jullien *Phys. Rev. Lett.* **51** 1123 (1983)
18. A A Tager, L K Kolmakova *Vysokomol. Soedin., Ser. A* **22** 483 (1980) [b]
19. F Family *J. Stat. Phys.* **36** 881 (1984)
20. G V Kozlov, K B Temiraev, V A Sozaev *Vestn. KBGU, Ser. Fiz. Nauk* **73** 24 (1999)
21. A Bunde, S Havlin *Fractals and Disordered Systems* (New York: Academic Press, 1996)
22. L V Dubrovina, S S Pavlova, T P Bragina *Vysokomol. Soedin., Ser. A* **30** 995 (1988) [b]
23. A P Karmanov, Yu B Monakov *Vysokomol. Soedin., Ser. B* **37** 328 (1995) [b]
24. V P Budtov *Fizicheskaya Khimiya Rastvorov Polimerov* (Physical Chemistry of Polymer Solutions) (St. Petersburg: Khimiya, 1992)
25. A A Askadskii *Struktura i Svoistva Teplostoikikh Polimerov* (The Structure and Properties of Heat-Resistant Polymers) (Moscow: Khimiya, 1981)
26. G V Kozlov, K B Temiraev, R A Shetov, A K Mikitaev *Materialovedenie* (2) 34 (1999)
27. G V Kozlov, K B Temiraev, G B Shustov *Izv. Vyssh. Uchebn. Zaved., Sev.-Kav. Region, Estestv. Nauki* (3) 82 (1998)
28. P Meakin, D Coniglio, H E Stanley, T A Witten *Phys. Rev. A, Gen. Phys., Ser. 3* **32** 2364 (1986)
29. P Pfeifer, D Avnir, D Farin *J. Stat. Phys.* **36** 699 (1984)
30. K B Temiraev, G V Shustov, G V Kozlov *Plast. Massy* (2) 30 (1999)
31. V N Shogenov, K B Temiraev, G V Kozlov, in *Fizika i Khimiya Perspektivnykh Materialov* (The Physics and Chemistry of Promising Materials) (Nal'chik: Kabardino-Balkarian State University, 1997)
32. V P Lebedev *Usp. Khim.* **47** 127 (1978) [*Russ. Chem. Rev.* **47** 69 (1978)]
33. H G E Hentschel, L M Deutch *Phys. Rev. A, Gen. Phys., Ser. 3* **29** 1609 (1984)
34. W D Brown, R C Ball *J. Phys. A* **18** (9) L517 (1985)
35. F S Barns *Biofizika* **41** 790 (1996)
36. M Kobayashi, T Yoshioka, M Imai, Y Itoh *Macromolecules* **28** 7376 (1995)
37. A G Kokorevich, Ya A Gravitis, V G Ozol'-Kalnin *Khim. Dreviciny* (1) 3 (1989)
38. T A Witten, P Meakin *Phys. Rev. B, Condens. Matter* **28** 5632 (1983)
39. R Jullien, R Boted, in *Fractals in Physics. Proceedings of the Sixth International Symposium on Fractals in Physics, ICTP, Trieste, Italy, 1985* (Eds L Pietronero, E Tosatti)
40. M Kolb *Physica A* **140** 416 (1986)

41. V V Korshak, S V Vinogradova, V A Vasnev *Vysokomol. Soedin., Ser. A* **10** 1329 (1968) [b]
42. D A Weitz, J S Huang, M Y Lin, J Sung *Phys. Rev. Lett.* **53** 1657 (1984)
43. S Alexander, R J Orbach *Phys. Lett.* **43** L625 (1982)
44. T A Vilgis *Physica A* **153** 341 (1988)
45. Yu G Yanovskii, D A Topchiev, V V Barancheeva, Yu A Malkanduev, V A Kabanov *Vysokomol. Soedin., Ser. A* **30** 1226 (1988) [b]
46. H G E Hentschel, J M Deutch, P Meakin *J. Chem. Phys.* **81** 2496 (1984)
47. M Muthukumar *J. Chem. Phys.* **83** 3161 (1985)
48. S M Aharoni *Macromolecules* **18** 2624 (1985)
49. N M Bityurin, V N Genkin, V P Zubov, M B Lachinov *Vysokomol. Soedin., Ser. A* **23** 1702 (1981) [b]
50. M Kolb, H J Herrmann *J. Phys. A* **18** (9) L435 (1985)
51. M Kolb, R Boted, R Jullien *Phys. Rev. Lett.* **53** 1653 (1984)
52. P Meakin, T Vicsek, F Family *Phys. Rev. B, Condens. Matter* **31** 564 (1985)
53. T Vicsek, F Family *Phys. Rev. Lett.* **52** 1669 (1984)
54. M V Shamurina, V I Roldugin, T D Pryamova, V V Vysotskii *Kolloid. Zh.* **57** 580 (1995)
55. R Botet, R Jullien *J. Phys. A* **17** 2517 (1984)
56. G V Kozlov, K B Temiraev, A Kh Malamatov *Khim. Promst* (4) 230 (1998)
57. D S Sanditov, G V Kozlov, V N Belousov, Yu S Lipatov *Ukr. Polym. J.* **1** 241 (1992)
58. G V Kozlov, V U Novikov, M A Gazaev, A K Mikitaev *Inzh.-Fiz. Zh.* **71** 241 (1998)
59. V A Beloshenko, G V Kozlov, Yu S Lipatov *Fiz. Tv. Tela* **36** 2903 (1994)
60. G V Kozlov, V U Novikov *Sinergetika i Fraktal'nyi Analiz Setchatykh Polimerov* (Synergetics and Fractal Analysis of Network Polymers) (Moscow: Klassika, 1998)
61. V S Ivanova *Sinergetika* (Synergetics) (Moscow: Nauka, 1992)
62. S Wu *J. Polym. Sci., Part B, Polym. Phys.* **27** 723 (1989)
63. G Careri *Ordine e Disordine Nella Materia* (Roma, 1982)
64. G V Kozlov, V A Beloshenko, M A Gazaev, V U Novikov *Mekhan. Kompozit. Mater.* **32** 270 (1996)
65. R F Boyer *Macromolecules* **25** 5326 (1992)
66. S Wu *Polym. Eng. Sci.* **30** 753 (1990)
67. R F Boyer, R L Miller *Macromolecules* **10** 1167 (1977)
68. G V Kozlov, V D Serdyuk, V A Beloshenko *Mekhan. Kompozit. Mater.* **30** 691 (1994)
69. G V Kozlov, V A Beloshenko, M A Gazaev, V N Varyukhin *Fiz. Tekhn. Vys. Davl.* **5** (1) 74 (1995)
70. V A Beloshenko, G V Kozlov, V N Varyukhin *Fiz. Tekhn. Vys. Davl.* **4** (2) 70 (1994)
71. G V Kozlov, V A Beloshenko, E N Kuznetsov, Yu S Lipatov *Dokl. Nat. Acad. Nauk Ukr.* (12) 126 (1994)
72. A S Balankin *Pis'ma Zh. Eksp. Teor. Fiz.* **17** (4) 84 (1991)
73. A S Balankin *Pis'ma Zh. Eksp. Teor. Fiz.* **15** (22) 15 (1989)
74. A S Balankin, A L Bugrimov *Vysokomol. Soedin., Ser. A* **34** 135 (1992) [b]
75. I I Perepechko, A V Maksimov *Vysokomol. Soedin., Ser. B* **31** 54 (1989) [b]
76. S M Aharoni *Macromolecules* **16** 1722 (1983)
77. V Novikov, M Gasaev, G Kozlov, in *Advances in Structural and Heterogeneous Continua (Abstracts of Reports of the Second Symposium)* (Moscow: Institute of Applied Mechanics of the Russian Academy of Sciences, 1995)
78. G V Kozlov, V U Novikov *Prikl. Fiz.* (1) 94 (1997)
79. V U Novikov, G V Kozlov *Materialovedenie,* (4) 6 (1997)
80. J Isaacson, T C Lubensky *J. Phys. Lett.* **41** L469 (1980)
81. A G Mikos, N A Peppas *J. Chem. Phys.* **88** 1337 (1988)
82. V U Novikov, G V Kozlov, M A Gazaev, A K Mikitaev *Povedenie Dissipativnykh Struktur v Deformirovannykh Polimernykh Matritsakh, Moskva, 1995* (Behaviour of Dissipative Structures in Deformed Polymer Matrices, Moscow, 1995); article deposited at the VINITI No 2944 (Moscow, 1995)
83. V U Novikov, G V Kozlov *Materialovedenie* (6–7) 42 (1997)
84. G V Kozlov, K B Temiraev,G B Shustov *Plast. Massy* (9) 27 (1998)
85. V N Shogenov, V N Belousov, V V Potapov, G V Kozlov, E V Prut *Vysokomol. Soedin., Ser. A* **33** 155 (1991) [b]
86. A S Balankin *Pis'ma Zh. Eksp. Teor. Fiz.* **16** (7) 14 (1990)
87. A S Balankin *Phys. Rev. B, Condens. Matter* **53** 5438 (1996)
88. A S Balankin, A D Izotov, V B Lazarev *Neorg. Mater.* **29** 451 (1993) [c]
89. V U Novikov, G V Kozlov, in *Fraktaly i Prikladnaya Sinergetika (Tez. Dokl. 1-go Mezhdistsiplinarnogo Seminara)* [Fractals and Applied Synergetics (Abstracts of Reports of the First Interdisciplinary Seminar)] (Moscow: Institute of Metallurgy, Russian Academy of Sciences, 1999) p. 124
90. G V Kozlov, V A Beloshenko, V N Varyukhin, M A Gazaev *Prikl. Mekhan. Tekhn. Fiz.* (39) 160 (1998)
91. A S Balankin *Pis'ma Zh. Eksp. Teor. Fiz.* **17** (11) 9 (1991)
92. V U Novikov, G V Kozlov *Fraktal'nyi Analiz Protsessov Razrusheniya Polimerov i Polimernykh Kompozitov* (Fractal Analysis of the Processes of Fracture of Polymer and Polymer Composites) (Moscow: Klassika, 1998)
93. G V Kozlov, V A Beloshenko, V N Varyukhin *Prikl. Mekhan. Tekhn. Fiz.* (37) 115 (1996)
94. G V Kozlov, V A Beloshenko, M A Gazaev, Yu S Lipatov *Vysokomol. Soedin., Ser. A* **38** 1423 (1996) [b]
95. G V Kozlov, V N Belousov, A K Mikitaev, N I Shustov *Dokl. Adygeiskoi (Cherkesskoi) Mezhdunar. Akad. Nauk* (2) 94 (1997)
96. P W Schmidt, A Höhr, H-B Neumann, H Kaiser, D Avnir, J S Lin *J. Chem. Phys.* **90** 5016 (1989)
97. R N Haward *Macromolecules* **26** 5860 (1993)
98. G V Kozlov, E N Kuznetsov, V A Beloshenko, Yu S Lipatov *Dokl. Nat. Akad. Nauk Ukr.* (11) 102 (1995)
99. G V Kozlov,V A Beloshenko,E N Kuznetsov, Yu S Lipatov *Ukr. Khim. Zh.* **63** 52 (1997)
100. V A Beloshenko, G V Kozlov,E N Kuznetsov,I V Stroganov, V F Stroganov *Fiz. Tekhn. Vys. Davl.* **7** 62 (1997)
101. S N Zhurkov *Fiz. Tv. Tela* **25** 3119 (1983)
102. V A Petrov *Fiz. Tv. Tela* **25** 3124 (1983)
103. V I Vettegren' *Fiz. Tv. Tela* **26** 1699 (1984)
104. G V Kozlov, V U Novikov *Materialovedenie* (8–9) 3 (1997)
105. G V Kozlov, A K Mikitaev, in *Polikondensatsionnye Protsessy i Polimery* (Polycondensation Processes and Polymers) (Nal'chik: Kabardino-Balkarian State University, 1988) p. 3
106. G V Kozlov, A K Mikitaev *Vysokomol. Soedin., Ser. B* **30** 520 (1988) [b]
107. V N Shchogenov, G V Kozlov, M A Gazaev, M Sh Kardanova, A K Mikitaev *Plast. Massy* (8) 32 (1986)
108. H H Kausch *Polymer Fracture* (Berlin: Springer, 1978)
109. G V Kozlov, K B Temiraev, V A Sozaev *Zh. Fiz. Khim.* **73** 727 (1999) [d]
110. G V Kozlov, K B Temiraev, G B Shustov, A K Mikitaev, in *XVI Mendeleevskii S'ezd po Obshchei i Prikladnoi Khimii (Tez. Dokl.)* [The XVIth Mendeleev Congress on General and Applied Chemistry (Abstracts of Report)] (Moscow: Research and Industrial Publisher's Union, Institute of Organic Chemistry, Russian Academy of Sciences, 1998) Vol. 2, p. 335
111. N I Mashukov, K B Temiraev, G B Shustov, G V Kozlov, in *The 6th International Workshop of Polymer Reaction Engineering (Abstracts of Reports), Berlin, 1998* p. 429
112. G V Kozlov, K B Temiraev, A Kh Malamatov *Khim. Promst* (4) 230 (1998)
113. P J Flory *Pure Appl. Chem.* **56** 305 (1984)
114. S T B Petrie *J. Macromol. Sci. Phys. B* **12** 225 (1976)
115. Ya I Frenkel' *Kineticheskaya Teoriya Zhidkostei* (Kinetic Theory of Liquids) (Moscow; Leningrad: Izd. Akad. Nauk SSSR, 1945)
116. E W Fischer, M Dettenmaier *J. Non-Cryst. Solids* **31** 181 (1987)
117. V A Bershtein, V M Egorov *Differentsial'naya Skaniruyushchaya Kalorimetriya v Fizikokhimii Polimerov* (Differential Scanning Calorimetry in Physical Chemistry of Polymers) (Leningrad: Khimiya, 1990)
118. Yu S Lipatov *Usp. Khim.* **47** 332 (1978) [*Russ. Chem. Rev.* **47** 186 (1978)]
119. D S Sanditov, G M Bartenev *Fizicheskie Svoistva Neuporyadochennykh Struktur* (Physical Properties of Disordered Structures) (Novosibirsk: Nauka, 1982)
120. V U Novikov, G V Kozlov *Prikl. Fiz.* (1) 50 (1998)
121. D S Sanditov, G V Kozlov, V N Belousov, Yu S Lipatov *Fiz. Khim. Stekla* **20** 3 (1994)

122. N I Mashukov, V D Serdyuk, G P Gladyshev, G V Kozlov *Vopr. Oboronnoi Tekhn.* **15** (97) 11 (1991)
123. D S Sanditov, G V Kozlov *Vysokomol. Soedin., Ser. A* **38** 1389 (1996) [b]
124. I C Sanchez *J. Appl. Phys.* **45** 4204 (1974)
125. B M Smirnov *Usp. Fiz. Nauk* **149** 177 (1986) [e]
126. E I Shemyakin *Dokl. Akad. Nauk SSSR* **300** 1090 (1988) [a]
127. A S Balankin *Pis'ma Zh. Eksp. Teor. Fiz.* **17** (4) 68 (1991)
128. G V Kozlov, V N Belousov, D S Sanditov, A K Mikitaev *Izv. Vyssh. Uchebn. Zaved., Sev.-Kav. Region, Estestv. Nauki* (1 – 2) 64 (1994)
129. D S Sanditov, G V Kozlov *Fiz. Khim. Stekla* (19) 593 (1993)
130. D S Sanditov, V V Mantatov *Vysokomol. Soedin., Ser. B* **32** 869 (1990) [b]
131. G V Kozlov, R A Shetov, A K Mikitaev *Dokl. Akad. Nauk SSSR* **290** 885 (1986) [f]
132. A S Balankin *Dokl. Akad. Nauk SSSR* **319** 1098 (1991) [a]
133. N I Mashukov, O A Vasnetsova, A Kh Malamatov, G V Kozlov *Lakokrasochn. Mater. Ikh Prim.* (1) 16 (1992)
134. P Pfeifer, D Avnir *J. Chem. Phys.* **79** 3558 (1983)
135. D Avnir, D Farin, P Pfeifer *J. Chem. Phys.* **79** 3566 (1983)
136. J E Kluin, Z Yu, S Vleeshouwers, J D McGervey, A M Jamieson, R Simha *Macromolecules* **24** 5089 (1992)
137. Q Deng, C S Sundar, Y C Jean *J. Phys. Chem.* **96** 492 (1992)
138. Z Yu, U Yahsi, J D McGervey, A M Jamieson, R Simha *Polym. Sci., Part B, Polym. Phys.* **32** 2637 (1994)
139. Q Deng, F Zandiehnadem, Y C Jean *Macromolecules* **25** 1090 (1992)
140. Y Y Wang, H Nakanishi, Y C Jean, T C Sandreczki *J. Polym. Sci., Part B, Polym. Phys.* **28** 1431 (1990)
141. W-C Yu, C S P Sung *Macromolecules* **21** 365 (1988)
142. V A Beloshenko, G V Kozlov, V N Varyukhin, V G Slobodina *Acta Polym.* **48** 181 (1997)
143. G V Kozlov, V A Beloshenko, V N Varyukhin *Ukr. Fiz. Zh.* **41** 218 (1996)
144. C L Wang, B Wang, S Q Li, S J Wang *J. Phys., Condens. Matter* **5** 7515 (1993)
145. G M Bartenev, Yu V Zelenev *Relaksatsionnye Yavleniya v Polimerakh* (Relaxation Effects in Polymers) (Leningrad: Khimiya, 1972)
146. G M Bartenev, Yu V Zelenev *Fizika i Mekhanika Polimerov* (The Physics and Mechanics of Polymers) (Moscow: Khimiya, 1983)
147. V S Dotsenko *J. Phys. C, Solid State Phys.* **18** 6023 (1985)
148. G V Kozlov, V A Beloshenko, I V Stroganov, Yu S Lipatov *Dokl. Nat. Acad. Nauk Ukrainy* (10) 117 (1995)
149. L Pietronero, E Tosatti (Eds), in *Fractals in Physics. Proceedings of the Sixth International Symposium on Fractals in Physics, ICTP, Trieste, Italy, 1985*
150. G V Kozlov, V A Beloshenko, Yu S Lipatov *Ukr. Khim. Zh.* **64** 56 (1998)
151. A S Balankin, A L Bugrimov, G V Kozlov, A K Mikitaev, D S Sanditov *Dokl. Akad. Nauk* **326** 463 (1992) [a]
152. G V Kozlov, V A Beloshenko, V A Lipskaya *Ukr. Fiz. Zh.* **41** 22 (1996)
153. B D Sanditov, V V Mantatov, G V Kozlov, V U Novikov, in *Baikal'skie Chteniya po Matematicheskomu Modelirovaniyu Protsessov v Sinergeticheskikh Sistemakh (Tez. Dokl. Vseros. Konf.), Ulan-Ude, 1999* [Baikal Reading on Mathematical Modelling of Processes in Synergetic Systems (Abstracts of Reports of the All-Russian Conference), Ulan-Ude, 1999] p. 36
154. G V Kozlov, V A Beloshenko, V N Varyukhin, Yu S Lipatov *Polymer* **40** 1045 (1999)
155. G V Kozlov, V U Novikov, A K Mikitaev, in *Sinergetika (Tez. Dokl.), Moskva, 1996* [Synergetics (Abstracts of Reports), Moscow, 1996] p. 226
156. V A Beloshenko, G V Kozlov *Mekhan. Kompozit. Mater.* **30** 451 (1994)
157. V A Beloshenko, G V Kozlov, V G Slobodina, E V Prut, V G Grinev *Vysokomol. Soedin., Ser. B* **37** 1089 (1985) [b]
158. G V Kozlov, V A Beloshenko, V G Slobodina, E V Prut *Vysokomol. Soedin., Ser. B* **38** 1056 (1996) [b]
159. J G Williams, G P Marshall *Proc. R. Soc. London, A Math. Phys. Sci.* **342** 55 (1975)
160. G V Kozlov, R A Shetov, A K Mikitaev *Vysokomol. Soedin., Ser. A* **29** 62 (1987) [b]
161. A Levene, W J Pullen, J Roberts *J. Polym. Sci., Part A-2* **3** 697 (1965)
162. I M Sokolov *Usp. Fiz. Nauk* **150** 221 (1986) [e]
163. L I Manevich, V G Oshmyan, M I Gai, E L Akopyan, N S Enilokopyan *Dokl. Akad. Nauk SSSR* **289** 128 (1986) [a]
164. A Margolina, S Wu *Polymer* **29** 2170 (1988)
165. N I Mashukov, V D Serdyuk, V N Belousov, G V Kozlov, M A Khatsukova *Fluktuatsionnaya Setka Molekulyarnykh Zatseplenii kak Perkolyatsionnaya Sistema, Moskva, 1994* (Fluctuation Network of Molecular Entanglements as a Percolation System, Moscow, 1994); article deposited at the VINITI No 1537 (Moscow, 1994)
166. G V Kozlov, M A Gazaev, V U Novikov, A K Mikitaev *Pis'ma Zh. Techn. Fiz.* **22** (16) 31 (1996)
167. V A Bagryanskii, V K Malinovskii, V N Novikov, L M Pushchaeva, A P Sokolov *Fiz. Tv. Tela* **30** 2360 (1988)
168. P Meakin, I Majid, S Halvin, H E Stanley *J. Phys. A* **17** L975 (1984)
169. J L McCauley *Int. J. Mod. Phys. B* **3** 821 (1989)
170. V U Novikov, G V Kozlov *Materialovedenie* (12) 8 (1999)
171. S Matsuoka, C J Aloisio, H E Bair *J. Appl. Phys.* **44** 4265 (1973)
172. Ma Zhenyi, S C Langford, J T Dickinson, M H Engelhard, D R Baer *J. Mater. Res.* **6** 183 (1991)
173. G V Kozlov, D S Sanditov *Angarmonicheskie Effekty i Fiziko-Mekhanicheskie Svoistva Polimerov* (Anharmonic Effects and Physical Mechanical Properties of Polymers) (Novosibirsk: Nauka, 1994)
174. T A Vilgis *J. Phys. (France),* **49** 1481 (1988)
175. G V Kozlov, V A Beloshenko, V N Varyukhin *Ukr. Fiz. Zh.* **43** 322 (1998)
176. G V Kozlov, V N Shogenov, A K Mikitaev *Inzh.-Fiz. Zh.* **71** 1012 (1998)
177. V N Belousov, G V Kozlov, A K Mikitaev, Yu S Lipatov *Dokl. Akad. Nauk SSSR* **313** 630 (1990) [a]
178. J T Colvin, H J Stapleton *J. Chem. Phys.* **82** 4699 (1985)
179. R M Brady, R C Ball *Nature (London)* **309** 225 (1984)
180. T A Witten, L M Sander *Phys. Rev. B, Condens. Matter* **27** 5686 (1983)
181. P Meakin, T A Witten *Phys. Rev. A, Gen. Phys., Ser. 3* **28** 2985 (1983)
182. M G Zemlyanov, V K Malinovskii, V N Novikov, P P Parshin, A P Sokolov *Zh. Eksp. Teor. Fiz.* **101** 284 (1992)
183. V K Malinovsky, V N Novikov *J. Phys. Condens. Matter* **4** L139 (1992)
184. A N Bobryshev, V N Kozomazov, L O Babin, V I Solomatov *Sinergetika Kompozitsionnykh Materialov* (The Synergetics of Composite Materials) (Lipetsk: Research and Industrial Union 'Orius', 1994)
185. V N Belousov, V A Beloshenko, G V Kozlov, Yu S Lipatov *Ukr. Khim. Zh.* **62** 62 (1996)
186. P Meakin *Phys. Rev. A, Gen. Phys., Ser. 3* **27** 1495 (1983)
187. M N Litt, P J Koch, A V Tobolsky *J. Macromol. Sci. Phys. B* **1** 587 (1967)
188. D C Prevorsek, B T De Bona *J. Macromol. Sci. Phys. B* **19** 605 (1981)
189. G V Kozlov, M A Gazaev, V U Novikov, A K Mikitaev *Fraktal'naya Fizika Formirovaniya Topologii i Struktury Polimerov, Moskva, 1995* (Fractal Physics of the Formation of Topology and Structure of Polymers, Moscow, 1995); article deposited at the VINITI No 3072 (1995)
190. T C Lubensky, J J Isaacson *Phys. Rev. A, Gen. Phys., Ser. 3* **20** 2130 (1979)
191. A T Dibenedetto, K L Trachte *J. Appl. Polym. Sci.* **14** 2249 (1970)
192. G V Kozlov, M A Gazaev, V A Beloshenko, V N Varyukhin, V G Slobodin *Ukr. Khim. Zh.* **61** 883 (1995)
193. G V Kozlov, V A Beloshenko, M A Gazaev *Ukr. Fiz. Zh.* **41** 1110 (1996)
194. G P Gladyshev, D P Gladyshev *Zh. Fiz. Khim.* **68** 790 (1994) [d]
195. G V Kozlov, V A Beloshenko, V N Varyukhin, V U Novikov *Zh. Fiz. Issl.* (1) 204 (1997)
196. G V Kozlov, V U Novikov *Prikl. Fiz.* (1) 85 (1997)
197. D J Bergman, Y Kantor *Phys. Rev. Lett.* **53** 511 (1984)

198. V N Belousov, G V Kozlov, N I Mashukov, Yu S Lipatov *Dokl. Akad. Nauk* **328** 706 (1993) [a]
199. V D Serdyuk, P N Kosa, G V Kozlov *Fiz. Tekhn. Vys. Davl.* **5** (3) 37 (1995)
200. F B Mosolov, O Yu Dinariev *Probl. Prochn.* (1) 3 (1988)
201. B L Cox, S J Wang *Fractals* **1** 87 (1993)
202. S Havlin, D Ben-Avraham *Phys. Rev. A, Gen. Phys., Ser. 3* **26** 1728 (1982)
203. B B Mandelbrot, D E Passoja, A J Pullax *Nature (London)* **308** 721 (1984)
204. C S Pande, L E Richards, N Louat B D Dempsey, A J Sahwoeble *Acta Met.* **35** 1633 (1987)
205. C W Lung, Z Q Mu *Phys. Rev. B, Condens. Matter* **38** 11781 (1988)
206. Z H Huang, J F Tian, Z G Wang *Scr. Met. Mater.* **24** (6) 967 (1990)
207. Z G Wang, D L Chen, X X Jiang *Scr. Met. Mater.* **24** (6) 827 (1990)
208. E E Underwood, K Banerji *Mater. Sci. Eng.* **80** 1 (1986)
209. Z Q Long, Jun Chen, Jizhi Chen *Theor. Appl. Fract. Mech.* **17** 157 (1992)
210. K Wright, B Karlsson *Microscopy* **129** 185 (1983)
211. B Dubuc, J F Quinion, C Roques-Carmes *Phys. Rev. A, Gen. Phys., Ser. 3* **39** 1500 (1989)
212. J J Mecholsky, D E Passoja, K S Feinberg-Ringel *J. Am. Ceram. Soc.* **72** 60 (1988)
213. G V Vstovskii, Candidate Thesis in Physical Mathematic Sciences, Institute of Metallurgy Academy of Sciences of the USSR, Moscow, 1990
214. T Kliser, M Bosek *Z. Met.kd.* **77** 582 (1986)
215. I R Göbel *Z. Met.kd.* **82** 858 (1991)
216. E E Underwood, K K Banerji, in *Metals Handbook* (New York: American Society of Metallurgy, 1992), Vol. 12, p. 211
217. P Meakin *Phys. Rep.* **235** 189 (1993)
218. A S Balankin *Rev. Mex. Fis.* **43** 545 (1997)
219. A S Balankin *Int. J. Fract.* **76** R63 (1995)
220. A S Balankin *Phys. Lett. A* **210** 51 (1996)
221. A V Neimark *Pis'ma Zh. Eksp. Teor. Fiz.* **51** 535 (1990)
222. K K Linger (Ed.) *Characterisation of Porous Solids* (Amsterdam: Elsevier, 1988)
223. V S Ivanova, A A Shanyavskii *Kolichestvennaya Fraktografiya* (Quantitative Fractography) (Chelyabinsk: Metallurgiya, 1988)
224. D W Schaefer, E J Martin, P Wiltzius, D S Cannel *Phys. Rev. Lett.* **52** 2371 (1984)
225. D Anvir, D Farin, P Pfeifer *Nature (London)* **308** 261 (1984)
226. P Pfeifer, D Anvir, D Farin *Surf. Sci.* **126** 569 (1983)
227. P Pfeifer, D Anvir, D Farin *J. Stat. Phys.* **36** 699 (1984)
228. A Neimark *Physica A* **181** 258 (1992)
229. E Bouchaud *Solid State Phenom.* **35**–**36** 353 (1994)
230. A Imre, T Pajkossy, L Nyikos *Acta Metall. Mater.* **40** 1819 (1992)
231. J Kappraff *Connections. The Geometric Bridge Between Art and Science* (New York: McGraw-Hill, 1991)
232. A S Balankin *Eng. Fract. Mech.* **57** 135 (1997)
233. R Xie, B Yang, B Jiang *Phys. Rev. B, Condens. Matter* **50** 3636 (1994)
234. B Chu, C Wu, D Wu, J C Phillips *Macromolecules* **20** 2642 (1987)
235. P Meakin, H E Stanley *Phys. Rev. Lett.* **51** 1457 (1984)
236. G R Dobson, M Gordon *J. Chem. Phys.* **41** 2389 (1964)
237. A Bunde, Sh Halvin (Eds) *Fractals in Science* (New York: Springer, 1994)
238. H D Bale, P W Schmidt *Phys. Rev. Lett.* **53** 596 (1984)
239. D W Schaefer, K D Keefer *Phys. Rev. Lett.* **53** 1383 (1984)
240. D N Winslow *Cement Conc. Res.* **15** 817 (1985)
241. T Freltoft, J K Kjems, S K Sinha *Phys. Rev. B, Condens. Matter* **33** 269 (1986)
242. C A Spence, S R Elliott *Solid State Commun.* **70** 1035 (1989)
243. V M Castano, G Martinez, J L Aleman, A Jimenez *J. Mater. Sci. Lett.* **9** 1115 (1990)
244. I Narisava *Prochnost' Polimernykh Materialov* (Strength of Polymeric Materials) (Translated into Russian; Moscow: Khimiya, 1987)
245. A Guinier, G Fournet *Small-Angle Scattering of X-Rays* (New York; London: Plenum, 1955)
246. D S Sanditov, M A Gazaev, G V Kozlov, A K Mikitaev, in *Zhidkost'. Problemy i Resheniya (Tez. Dokl. 2-i Regional'noi Konf)* [Liquid. Problems and Solutions (Abstracts of Reports of the Second Regional Conference)] (Novosibirsk: Novosibirsk State University, 1996) p. 46
247. A Blumen, J Manz *J. Chem. Phys.* **71** 4694 (1979)
248. P Wiltzius *Phys. Rev. Lett.* **58** 710 (1987)

[a] — *Dokl. Chem. Technol., Dokl. Chem. (Engl. Transl.)*
[b] — *Polym. Sci. (Engl. Transl.)*
[c] — *Inorg. Mater. (Engl. Transl.)*
[d] — *Russ. J. Phys. Chem. (Engl. Transl.)*
[e] — *Physics-Uspekhi (Engl. Transl.)*